

# Global silicate weathering and CO<sub>2</sub> consumption rates deduced from the chemistry of large rivers

J. Gaillardet <sup>a,\*</sup>, B. Dupré <sup>b</sup>, P. Louvat <sup>a</sup>, C.J. Allègre <sup>a</sup>

<sup>a</sup> *Laboratoire de Géochimie et Cosmochimie, UMR CNRS 7579, Institut de Physique du Globe, Université de Paris 7, 4 Place Jussieu, 75252 Paris Cedex 05, France*

<sup>b</sup> *Laboratoire de Géochimie, OMP, UMR-CNRS 5563, 38 rue des 36 ponts, 31400 Toulouse, France*

Received 28 November 1997; received in revised form 8 May 1998; accepted 16 July 1998

## Abstract

The main problem associated with the study of silicate weathering using river dissolved load is that the main control of solute chemistry is lithology and that all rivers are influenced by carbonate and evaporite weathering. In this paper, newly compiled data on the 60 largest rivers of the world are used to calculate the contribution of main lithologies, rain and atmosphere to river dissolved loads. Technically, an inverse method is used to solve a model containing of a series of mass budget equations relating river concentrations to chemical weathering products and atmospheric inputs. New estimates of global silicate weathering fluxes and associated CO<sub>2</sub> consumption fluxes are given. The role of basalt weathering on oceanic islands and volcanic arcs is emphasized. For each large river, an attempt is made to calculate chemical weathering rates of silicates per unit area. Only relative chemical weathering rates can be calculated. The relationships between the chemical weathering rates of silicates and the possible controlling parameters are explored. A combined effect of runoff-temperature and physical denudation seems to explain the variability of modern silicate chemical weathering rates. The results of this study highlight the coupling between the physical and the chemical processes of silicate weathering. Only an active physical denudation of continental rocks seems to be able to maintain high chemical weathering rates and significant CO<sub>2</sub> consumption rates. © 1999 Elsevier Science B.V. All rights reserved.

**Keywords:** Silicate weathering; CO<sub>2</sub> consumption; Large rivers

## 1. Introduction

On the continents, two major processes act as sinks for atmospheric carbon: the uptake of CO<sub>2</sub> during rock weathering and transformation to dissolved HCO<sub>3</sub><sup>-</sup> in continental waters and the uptake

of the CO<sub>2</sub> during photosynthesis and transformation to organic matter. One of the major goals of river geochemistry studies is to estimate the present-day inorganic and organic denudations of the continents and their associated CO<sub>2</sub> consumption.

This paper focuses on the consumption of atmospheric CO<sub>2</sub> through rock weathering (mainly carbonate and silicate weathering). Since the pioneering work of Garrels and Mackenzie (1971) many studies have focused on river geochemistry, following two

\* Corresponding author. Fax: +33-144-27-37-52; e-mail: gaillardet@ipgp.jussieu.fr

Table 1

Basins	Area (10 <sup>6</sup> km <sup>2</sup> )	Discharge (km <sup>3</sup> yr <sup>-1</sup> )	Runoff (mm yr <sup>-1</sup> )	TDS (mg l <sup>-1</sup> )	TSS (mg l <sup>-1</sup> )	Na (μmol l <sup>-1</sup> )	K (μmol l <sup>-1</sup> )	Ca (μmol l <sup>-1</sup> )	Mg (μmol l <sup>-1</sup> )	Cl (μmol l <sup>-1</sup> )	SO <sub>4</sub> (μmol l <sup>-1</sup> )	HCO <sub>3</sub> (μmol l <sup>-1</sup> )	SiO <sub>2</sub> (μmol l <sup>-1</sup> )	Sr (μmol l <sup>-1</sup> )	<sup>87</sup> Sr/ <sup>86</sup> Sr
Amazon	6.112	6590	1078	44	182	80	21	135	37	61	47	344	115	0.19	0.71148
Changjiang	1.808	928	513	221	520	222	36	973	292	151	164	2311	108	2.42	0.71071
Mississippi	2.98	580	195	216	862	478	72	850	366	294	266	1902	127	1.71	0.71020
Irrawady	0.41	486	1185	201	535	1304	51	250	247	514	52	1967	167		
Ganges	1.05	493	470	182	1100	417	67	580	267	143	83	1951	128	1.02	0.72490
Danube	0.817	207	253	428	313	739	51	1473	1117	1509	660	3328	69	2.76	0.70890
Yenisei	2.59	620	239	112	23	226	26	413	152	271	104	939	138		
Salween	0.325	211	649	306		435	26	1150	658	571	10	3475			
Mackenzie	1.787	308	172	209	134	330	26	890	337	226	369	1803	50	2.00	0.71100
St. Lawrence	1.02	337	330	168	12	239	35	750	247	214	146	1656	40	1.40	0.70963
Lena	2.49	525	211	112	30	196	18	428	210	343	142	870	97		
Xijiang	0.437	363	831	161	190	117	31	810	198	91	85	1639	142	1.27	0.71068
Ob	2.99	404	135	126	40	230	26	465	210	186	89	1279	43		
Brahmaputra	0.58	510	879	101	1060	91	100	350	156	31	104	951	130	0.67	0.71970
Parana	2.783	568	204	86	139	231	94	173	86	185	21	690	285	0.52	0.71390
Mekong	0.795	467	587	263	321	663	48	1001	367	448	343	2305	167	3.39	0.71020
Congo–Zaire	3.698	1200	324	35	32	96	43	56	59	37	15	258	157	0.15	0.71918
Rhine	0.224	69.4	310	600		3957	164	2013	469	4943	771	2590	87	6.23	0.70920
Yukon	0.849	200	236	183	286	113	31	795	295	31	233	1787	128	1.59	0.71370
Orinoco	1.1	1135	1032	25	132	64	17	65	27	25	24	164	105	0.21	0.71830
Magdalena	0.235	237	1009	118	928	361	49	375	136	383	150	808	210		
Columbia	0.669	236	353	115	64	217	28	450	206	86	115	1033	150	0.98	0.71210
Indus	0.916	90	98	302	2778	1370	112	958	374	931	436	2130	233	3.69	0.71100
Weser	0.046	10.6	230	2463	31	24957	1077	1400	6214	35229	2448	2754	67	8.23	0.70890
Don	0.42	28.9	69	829	80	6348	26	2073	1481	4200	2240	3295	5		
Nelson	1.132	89.3	79	236		696	59	823	457	486	271	2115	23	0.86	0.71460
Godavari	0.313	105	335	193	1619	352	56	755	99	403	104	1721	352		
N. Dvina	0.348	110	316	173	43	217	26	750	296	154	403	1361	38		
Wisla	0.198	32.5	164	583	79	2696	126	2250	535	4200	792	3115		7.94	0.70940
Amur	1.855	344	185	55	72	126	26	223	95	66	65	477	36		

Huanghe	0.752	41	55	460	26900	2370	105	1175	848	1563	696	3361	128	13.00	0.71111
Rhone	0.0956	54	565	339	500	491	54	1770	267	640	479	2885	67	5.94	0.70870
Shatt el arab	0.5413	45.8	85	400	2295	1348	77	1300	905	914	760	2951	115		
Hong He	0.12	123	1025	147	1057	483	38	388	333	237	119	1328	167	1.55	0.71140
Po	0.07	46.7	667	354	330	730	77	1553	490	517	626	2918	67		
Fly	0.061	141	2311	116	816	101	11	533	72	3	28	1284	150		
Elbe	0.148	22.8	154	698	37	3717	669	2675	663	4971	1594	2164	67	6.53	0.70970
Tocantins	0.757	372	491	42	202	82	35	54	75	35	27	316	193	0.38	0.72067
Dnepr	0.504	54	103	274	40	609	26	1105	424	489	326	2502	57		
Sepik	0.0787	120	1525	114	68	152	10	388	165	14	47	1205	208		
Nile	2.87	83	10	388	1400	2261	200	775	576	1257	542	2852	213		
Narmada	0.102	39	382	285	3071	1522		625	790	486	52	2869	150		
Murray Darling	1.06	23.6	22	453	1271	4391	154	525	700	4886	396	1541	83		0.71380
Purari	0.0306	84.13	2749	126	951	139	26	515	107	34	25	1328	230		
Panuco	0.0663	17.3	261	601		1322	103	2750	1202	711	2333	2918			
Fraser	0.22	112	509	92	175	126	18	443	148	69	85	841	91	0.795	0.7112
Mahanadi	0.132	66	500	147	909	443	38	260	391	883	156	998	150		
Kolima	0.66	132	200	74	126	122	46	270	99	80	147	570	67		
Odra	0.112	18.3	163	529	7	2196	544	2150	535	3057	1052	2459			
Krishna	0.259	30	116	317	2130	1848	77	688	556	1057	656	2049	83		
Pechora	0.324	131	404	70	50	130	26	260	115	117	83	638	27		
Niger	1.2	154.1	128	59	260	78	28	138	78	26	5	549	233	0.25	0.71400
Ebro	0.084	17.4	207	517	86	3283	51	1875	646	2071	1391	2159	177		
Uruguay	0.24	145	604	60	76	123	35	148	99	57	52	426	250		
Kuskokwin	0.123	59.9	487	145	116	96	20	605	226	19	147	1469	127	1.06	0.70900
Cauveri	0.088	21	239	396		2609	141	700	988	1429	333	2902	317	3.62	0.71300
Zambese	1.33	103	77	80	194	235	49	265	169	186	31	525	280		
Khatanga	0.364	85.3	234	96	17	422	26	313	148	357	58	785	53		
Seine	0.0786	12.9	164	493	44	922	126	2625	379	1100	580	4131	106	3.84	0.70824
Nemanus	0.0982	19.6	200	447	34	687	26	1735	926	791	626	4075	34		
Kikori	0.0132	40.06	3035	177		57	5	933	165	9	11	2049	133		
Limpopo	0.44	26	59	238	1269	896	118	483	506	406	54	2361	295		

All data from the compilation of Meybeck and Ragu (1997), except Mekong (Dupré, unpublished data) and Indus (Pande et al., 1994). Sr isotopic ratios and Sr concentrations are derived from a number of sources (see text).

main and complementary approaches: small scale studies of rivers draining one rock type under a given climate (e.g., Amiotte-Suchet and Probst, 1993; Bluth and Kump, 1994; White and Blum, 1995; Gislason et al., 1996; Louvat and Allègre, 1997) or using the world largest rivers for a more global picture (Holland, 1978; Meybeck, 1979; Berner et al., 1983; Meybeck, 1987; Amiotte-Suchet and Probst, 1995). The major advantage of studying large rivers is that it gives global information, integrating over large portions of continental crust and varying climatic regions. It is remarkable that the 30 largest rivers of the world represent half of the total runoff to the ocean. However, the study of large rivers poses the problem that the dominant control of dissolved yields is clearly lithology (e.g., Edmond and Huh, 1997), which obscures any effect from the other parameters, for example climate. In this paper we present a new approach, allowing calculation of contributions of the different lithologies to the dissolved load of large rivers, also the associated chemical weathering and  $\text{CO}_2$  consumption rates. Previous attempts to decompose large river chemistry into rock weathering products has been made by Holland (1978), Meybeck (1979), Wollast and Mackenzie (1983) and Berner et al. (1983). All these papers applied more or less the method (we will say 'the direct method') initiated by Garrels and Mackenzie. This method is based on river chemistry data and consists of allocating each solute to the dissolution of a rock type following a series of steps (see, e.g., Meybeck, 1987). These studies were based either on the large river chemical data set of Livingstone (1963) or on that of Meybeck (1979). More recently, the 'Temperate Stream Model' of Meybeck (1987) proposed a new approach based on the composition of waters draining major rock types (in France; Meybeck, 1986) and their outcrop proportions at the surface of the Earth. Finally, Amiotte-Suchet and Probst (1995) refined this method by including a runoff dependence of weathering rates of major rock types and, through this, proposed a global estimate of atmospheric  $\text{CO}_2$  consumption by chemical erosion of continental rocks.

This paper consists of a generalization of a technique developed for the Congo and Amazon basin (Négrel et al., 1993; Gaillardet et al., 1997) to a new compilation of major world rivers. Compared to the

studies initiated by Garrels and Mackenzie (1971), our approach is also based on data, but is not a 'direct method' in the sense defined above. In this paper, a global mixing model between erosion products is postulated and the river data are used to constrain this model. This is basically an inverse method in the sense of geochemists and geophysicists.

## 2. Origin of data

Water discharges, drainage basin areas, temperatures, major dissolved ions and silica concentrations are taken from the recent GEMS/WATER Global Register of River Inputs (GEMS/GLORI) compiled by Meybeck and Ragu (1997). This data base compiles the water quality of about 550 rivers having exorheic basins exceeding  $10\,000\text{ km}^2$  and water discharges exceeding  $10\text{ km}^3\text{ yr}^{-1}$ . For the present study, the 60 world largest rivers ranked by decreasing dissolved load (in  $10^6\text{ t yr}^{-1}$ ) were selected (Table 1). The largest river in terms of dissolved discharge is the Amazon river ( $287 \times 10^6\text{ t yr}^{-1}$ ), the smallest, the Seine river ( $6.4 \times 10^6\text{ t yr}^{-1}$ ). Dissolved yields were calculated from total dissolved loads (calculated as sum of major element concentrations) and water discharges. For a number of rivers draining highly populated or cultivated areas (Mississippi, Indus, Don, Murray, Nile), actual discharges differ significantly from natural ones. For example, for the Nile river the natural discharge is  $83\text{ km}^3\text{ yr}^{-1}$ , while the actual is  $0.3\text{ km}^3\text{ yr}^{-1}$ . In such cases, the natural water discharges have been used. For the Mekong and Indus rivers other data set were preferred, respectively those of Dupré (unpublished data) and Pande et al. (1994).

The database presented in Table 1 covers a continental area of  $53.6 \times 10^6\text{ km}^2$  or about 54% of the exorheic continental area. The river having the lowest continental area is the Purari river, Papua N.G. ( $31\,000\text{ km}^2$ ). In terms of water discharge, the rivers listed in Table 1 represent  $19\,800\text{ km}^3\text{ yr}^{-1}$  or about 53% of the total water discharge to the ocean. On a global scale, total dissolved solids (TDS) values range from about  $30\text{ mg l}^{-1}$  (Orinoco, Congo–Zaire) to about  $800\text{ mg l}^{-1}$  (Don, Balsas, Elbe). One exception is the Weser river which has a particularly

high dissolved load ( $2463 \text{ mg l}^{-1}$ ). Table 1 shows that only nine rivers have a TDS value greater than  $500 \text{ mg l}^{-1}$  (Rhine, Weser, Don, Wisla, Elbe, Panuco, Odra, Ebro, Seine). Their high salinity is either due to aridity or pollution. Pollution is particularly apparent for the rivers of Northern Europe (Weser, Elbe, Rhine, Wisla, Odra or Seine) and for Don river ( $\text{Cl} > 1000 \mu\text{mol l}^{-1}$ ).

Sr concentrations and isotopic ratios have been compiled from different sources: Stordal and Wasserburg (1983) for the Mississippi, Wadleigh et al. (1985) for the Mackenzie, Palmer and Edmond (1989), Krishnaswami et al. (1992) for the Ganges–Brahmaputra, Négrel et al. (1993) for the Congo–Zaire river, Pande et al. (1994) for the Indus, Hieronymus et al. (1995) for the Tocantins, Cameron et al. (1995) for the Fraser river, Douglas et al. (1995) for the Murray river, Yang et al. (1996) for the St. Lawrence river, Roy et al. (1996) for China rivers, and Gaillardet et al. (1997) for the Amazon. It must be kept in mind that, conversely to major ions data, the Sr data do not represent multi-year average analysis but correspond generally to a simple sampling point.

Only 29 rivers can be characterized by their Sr isotopic ratios and some very large rivers such as the Irrawady, Salween, Magdalena are still unknown for their isotopic composition.

### 3. Methodology

Each river selected for this study can be characterized by a number of elemental ratios and a Sr isotopic composition. We focused on following the Na normalized molar ratios ( $\text{Ca}/\text{Na}$ ,  $\text{K}/\text{Na}$ ,  $\text{Mg}/\text{Na}$ ,  $\text{Cl}/\text{Na}$ ,  $\text{SO}_4/\text{Na}$ ,  $\text{HCO}_3/\text{Na}$  ratios). Instead of absolute concentrations (being dependent on dilution and evaporation processes), elemental ratios and isotopic compositions processes are intensive parameters that permit the comparison between rivers draining areas of high runoff (Amazon, Zaire, Orinoco) and rivers draining arid areas (Limpopo, Murray).

For the 60 largest rivers of the world, important variations are observed for elemental ratios and Sr isotopic compositions. The histograms (using a logarithmic scale on the X-axis) representing the distributions of elemental ratios in the 60 rivers of this

study are shown in Fig. 1. Most Na-normalized ratios fluctuate over three orders of magnitude, except for  $\text{Cl}/\text{Na}$  and  $\text{Mg}/\text{Na}$  ratios whose variations spread over two orders of magnitude. As frequently observed for geochemical distributions (Allègre and Lewin, 1995) the distributions of Fig. 1 appear to be log-normal. Most of the rivers have a  $\text{Ca}/\text{Na}$  ratio between 1 and 3,  $\text{HCO}_3/\text{Na}$  between 4 and 8,  $\text{Cl}/\text{Na}$  between 0.6 and 1,  $\text{SO}_4/\text{Na}$  between 0.25 and 0.5,  $\text{Mg}/\text{Na}$  between 0.5 and 1 and  $\text{K}/\text{Na}$  ratio between 0.25 and 0.4. The geochemical distribution of  $^{87}\text{Sr}/^{86}\text{Sr}$  in the 60 rivers of this study is presented Fig. 1 and displays a highly asymmetric histogram showing that most of rivers have an isotopic composition around 0.710.

The best correlations observed between elemental ratios are those between  $\text{Ca}/\text{Na}$  vs.  $\text{Mg}/\text{Na}$  ( $r = 0.82$   $n = 62$ ) and  $\text{Ca}/\text{Na}$  vs.  $\text{HCO}_3/\text{Na}$  ( $r = 0.98$ ,  $n = 62$ ). These correlations are shown in a log–log space in Fig. 2. The rivers having TDS values greater than  $500 \text{ mg l}^{-1}$  (polluted rivers of Europe, Ebro and Panuco) have been distinguished from the other large rivers. Similar correlations have been reported for the Congo and Amazon Basins (Négrel et al., 1993; Gaillardet et al., 1997). As discussed extensively in these previous papers, these correlations reflect mostly the mixture between two main water-types whose range of chemical composition is represented in Fig. 2.

- Waters draining carbonates show Ca and Mg dominated reservoirs. Numerous authors have reported chemical analysis of small rivers draining only carbonates (Stallard, 1980; Meybeck, 1986, 1987; Négrel et al., 1993). Once corrected from atmospheric inputs, all these small rivers have  $\text{Ca}/\text{Na}$  ratios close to 50,  $\text{Mg}/\text{Na}$  ratios close to 10,  $\text{HCO}_3/\text{Na}$  ratios close to 120 and  $\text{Sr}/\text{Na}$  ratios close to  $35 \times 10^{-3}$ .

- The end member having lower Na normalized ratios is that of waters draining silicates. The molar  $\text{Ca}/\text{Na}$  ratio of average crustal continental rocks is close to 0.6 (Taylor and McLennan, 1985), and due to the higher solubility of Na relative to Ca, lower  $\text{Ca}/\text{Na}$  molar ratio are expected in the dissolved load of rivers draining silicates. This is in agreement with the data from Stallard (1980), Meybeck (1986, 1987), Négrel et al. (1993), Edmond et al. (1994) and White and Blum (1995) for small streams drain-

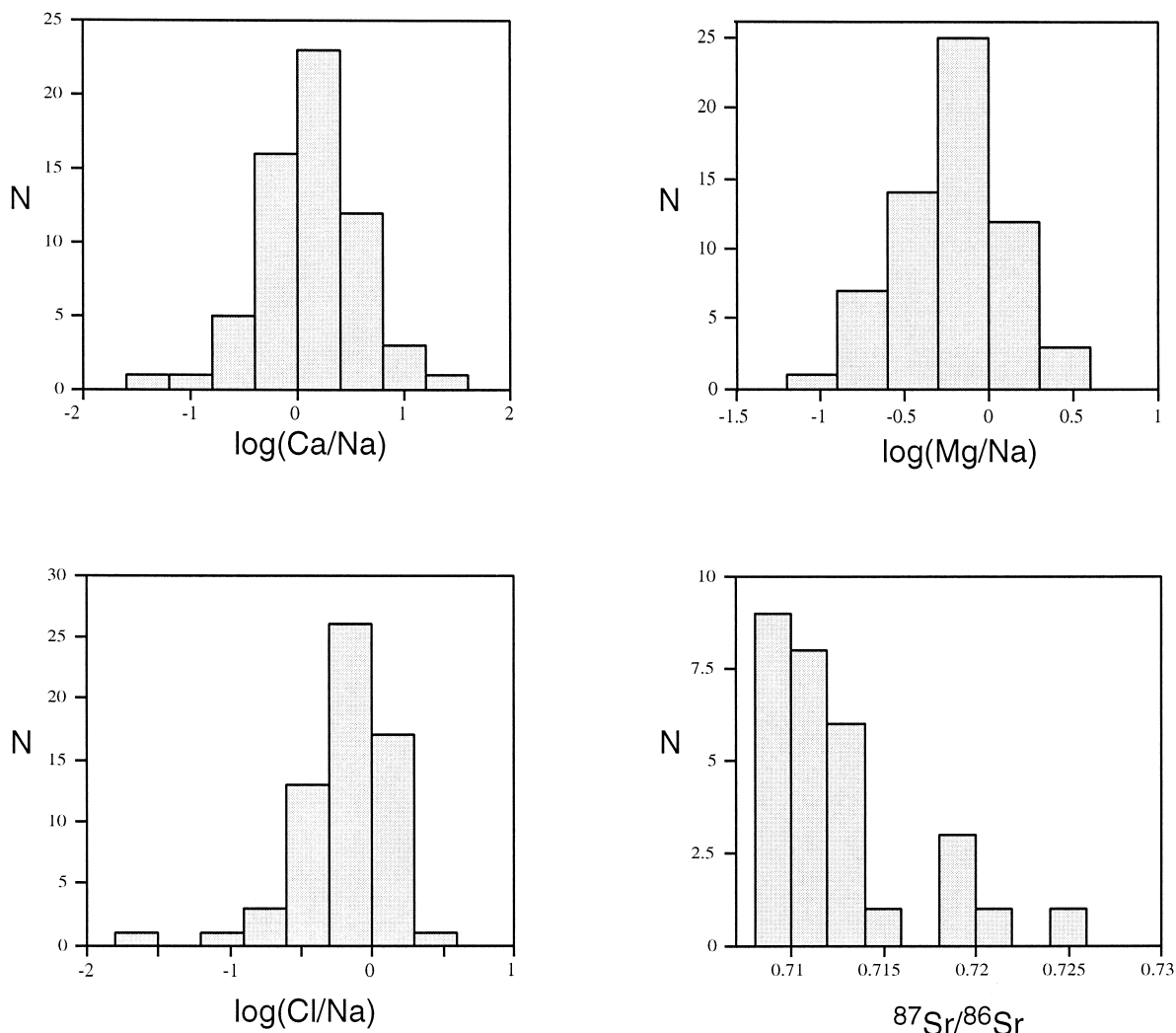


Fig. 1. Geochemical distributions of some Na-normalized molar ratios and isotopic ratios in the 60 largest rivers. The distributions of Ca/Na, Mg/Na and Cl/Na are log-normal distributions.

ing only rocks made of aluminosilicates. The histograms of Ca/Na molar ratios from the different data bases are plotted Fig. 3. Dissymmetrical distributions toward high Ca/Na values are observed for the streams of Western Europe and the streams sampled by White and Blum (mostly at temperate latitudes). We assign the following chemical composition to the silicate end member:  $\text{Ca}/\text{Na} = 0.35 \pm 0.15$ ,  $\text{Mg}/\text{Na} = 0.24 \pm 0.12$ ,  $\text{HCO}_3/\text{Na} = 2 \pm 1$ ,  $1000 * \text{Sr}/\text{Na} = 3 \pm 1$ . These values correspond to the modal values of the histograms (e.g., Fig. 3 for

the Ca/Na ratio). The existence of silicate draining rivers having higher Na-normalized ratios can be accounted for by at least three reasons:

- The source rocks have average Na-normalized ratios higher than average crustal rocks (0.6). This is clearly the case for the rivers draining the TTG rock system.
- The weathering conditions are such that Ca rich minerals are preferentially dissolved. It is particularly interesting that a symmetrical distribution for Ca/Na ratios (Fig. 3) is observed for the streams of

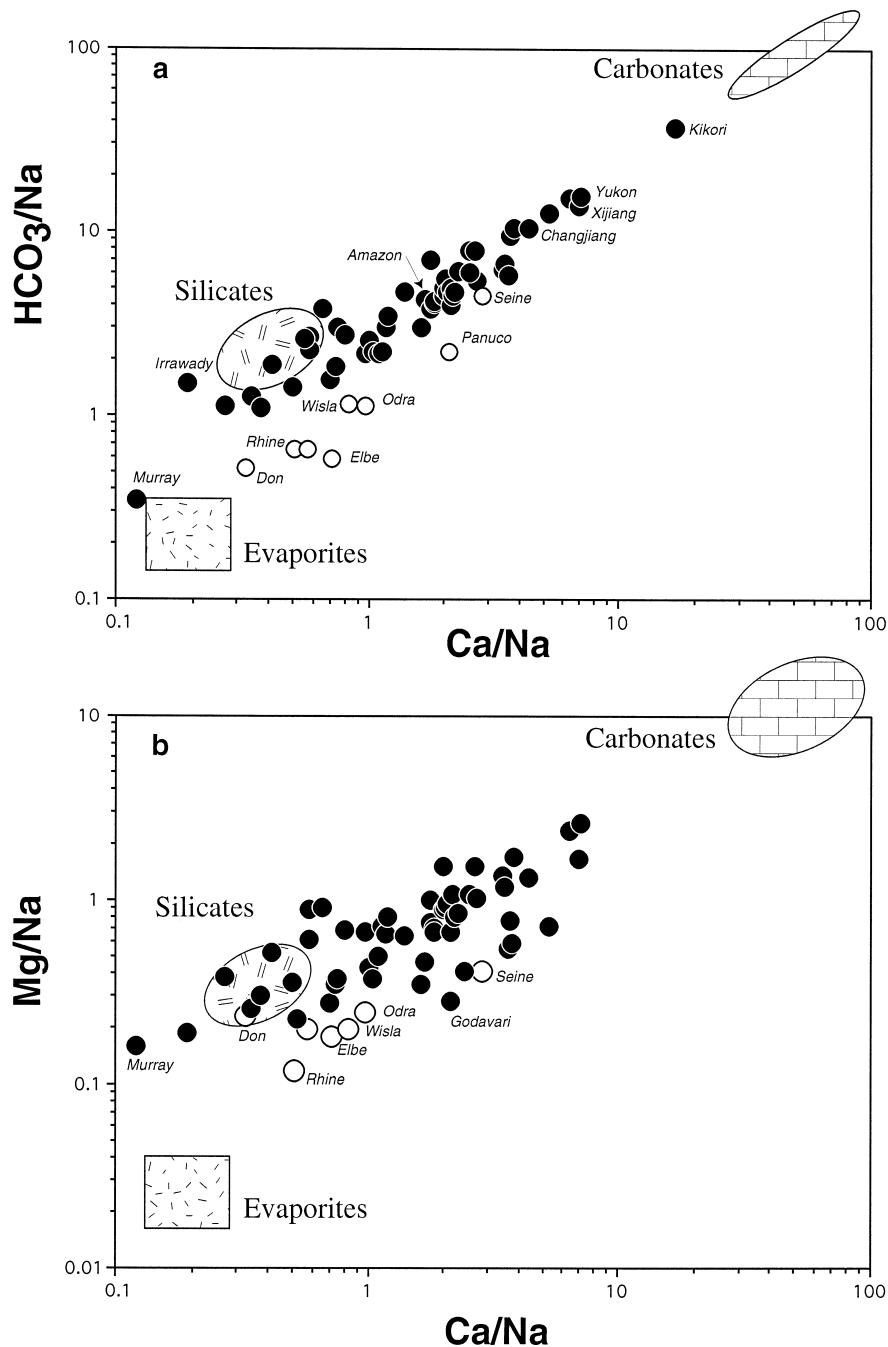
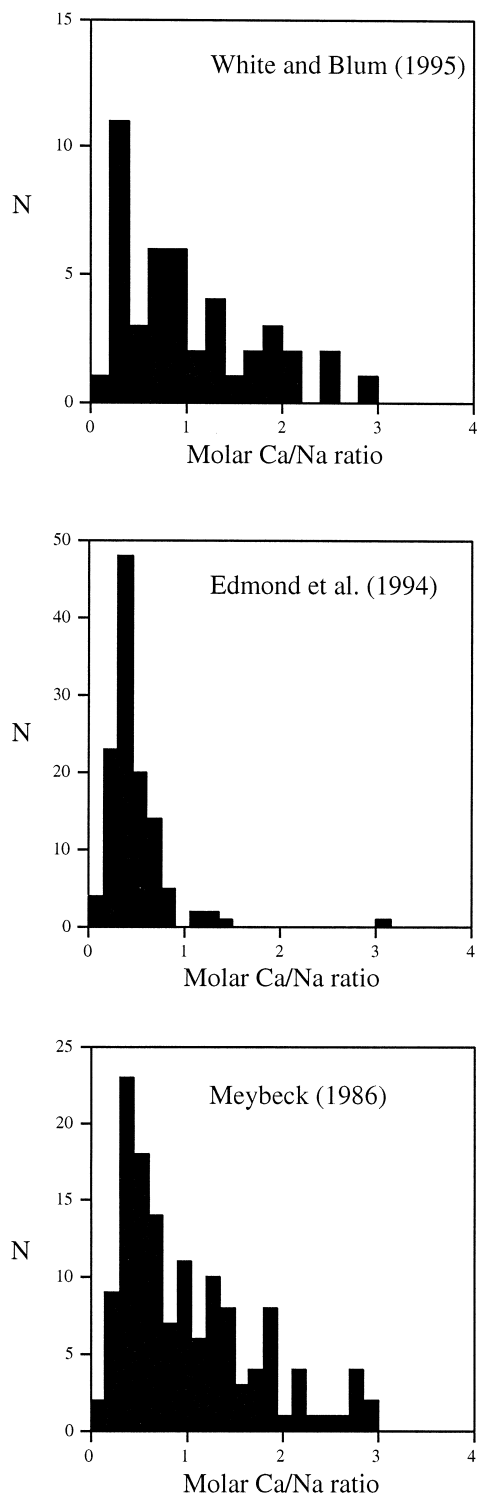


Fig. 2. Mixing diagrams using Na-normalized molar ratios in the dissolved phase of the 60 largest rivers. The rivers having TDS values greater than  $500 \text{ mg l}^{-1}$  (the most polluted rivers) have been distinguished (open circles) from the others. End member reservoirs were estimated using data on small rivers draining one single lithology (carbonates, silicates and evaporites, see text for references). The rainwater (marine) end member is not represented because of its very different chemical signature.



the Guyana shield where chemical weathering is intense (transport limited regime), while the studies of White and Blum or Meybeck, confined to upland small watersheds that all fell within the weathering-limited regime of weathering, exhibit dissymmetrical distributions. It is quite probable in such regions, that unweathered minerals (Na rich) are transported as streams sediments and weathered downstream. In this case, the sampling of small monolithological streams may not lead to a fair estimate of the chemical signature of the waters draining the silicate end member.

• Finally, the presence of disseminated calcite within the catchments can also explain the deviation observed toward high Ca/Na values. In our model, this calcite is included in the carbonate end member.

Although we clearly favor the above set of Na-normalized ratio for the chemical signature of the crustal silicate end member, a sensitivity analysis will be discussed using a set of higher ratios ( $\text{Ca/Na} = 1 \pm 0.4$ ,  $\text{Mg/Na} = 0.6 \pm 0.2$ ,  $\text{HCO}_3/\text{Na} = 3 \pm 1$  and  $\text{Sr/Na} = 5 \pm 2 \times 10^{-3}$ ). For rivers draining significant outcrops of volcanic rocks (Parana, Namada, rivers of Papua N.G.), the small river data of Benedetti et al. (1994) (Parana Basin), Meybeck (1986), Louvat and Allègre (1997) and Gislason et al. (1996) were used to constrain the following chemical signature of basalt-draining rivers:  $\text{Ca/Na} = 0.5 \pm 0.2$ ,  $\text{Mg/Na} = 0.5 \pm 0.2$ ,  $\text{HCO}_3/\text{Na} = 2 \pm 1$ ,  $1000 * \text{Sr/Na} = 5 \pm 2$ .

It is clear from Fig. 2 that the silicate and carbonate end members do not explain all the variability of the data and hence that other end members should exist. The most evident end member is rainwater. It is classically considered that Cl in rivers whose drainage does not contain any salty rocks or evaporites is derived from the atmosphere because common rocks do not contain significant amount of Cl. Cl is then used as an index for atmospheric inputs to

Fig. 3. Geochemical distributions of Na-normalized molar ratios measured by different authors in small streams draining granitoid rocks. The streams of White and Blum (1995) are mostly in North America and Europe and encompass significant climate differences. The data from Edmond et al. (1994) are limited to the wet tropical area of the Guyana shield. The data from Meybeck (1986) correspond to small streams in France.



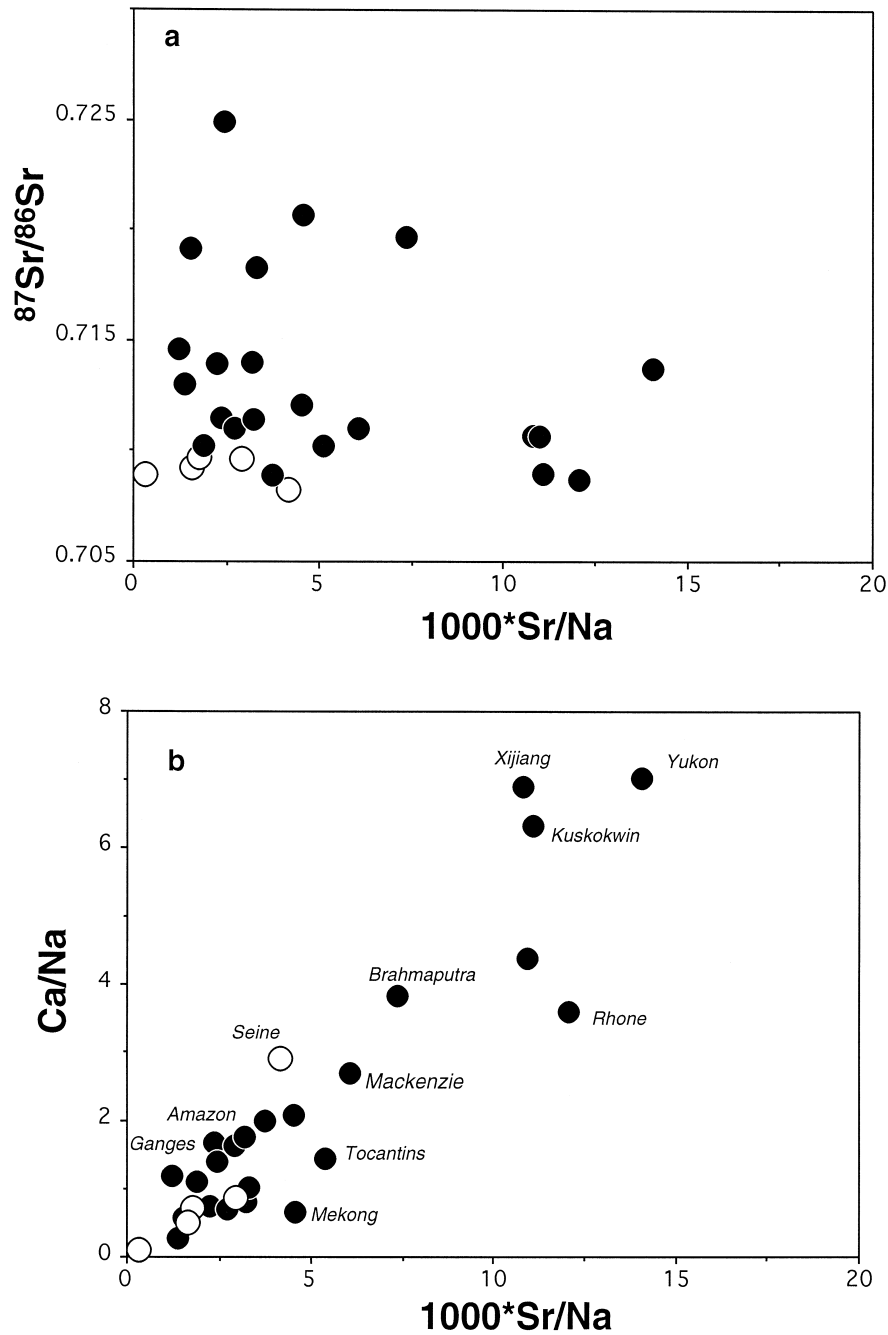


Fig. 4. (a) Mixing diagrams using Sr isotopic compositions in largest river waters and Sr/Na molar ratios. Open circles represent the most polluted rivers. (b) Global correlation between Ca/Na and Sr/Na ratios. Marine carbonates have isotopic compositions between 0.707 and 0.709, Ca/Na and Sr/Na molar ratios close to 50 and  $40 \times 10^{-3}$ , respectively. Evaporites have the same range of Sr isotopic composition but very low Sr/Na and Ca/Na ratios. Silicates draining waters have low Ca/Na ( $\pm 0.35$ ) and Sr/Na ratios ( $\pm 3 \times 10^{-3}$ ) and Sr isotopic composition from 0.705 for recent magmatic provinces up to 0.735 for old crustal segments.

ivers and the correction of sea salts inputs to rivers is deduced using the elemental ratios of seawater ( $\text{Cl}/\text{Na} = 1.15$ ,  $\text{Ca}/\text{Na} = 0.02$ ,  $\text{Mg}/\text{Na} = 0.11$ ,  $\text{HCO}_3/\text{Na} = 0.004$ ). As will be detailed later, atmospheric Cl concentrations in large rivers do not exceed  $30 \mu\text{mol l}^{-1}$ , except in arid areas. However, it is apparent from Table 1 that among the rivers from this study, only 10 (16%) have Cl concentrations lower than  $30 \mu\text{mol l}^{-1}$ .

For the remaining rivers, evaporites must be present in the basin. This end member is certainly the most difficult to be constrained because of the diversity of salt rock types. Few data are available in the literature for streams draining evaporites (Reeder et al., 1972; Stallard, 1980; Meybeck, 1984; Meybeck, 1986). Compiling these data sets (about 60 rivers), the most probable range of chemical composition for waters draining evaporites in  $\text{HCO}_3/\text{Na}$  or  $\text{Mg}/\text{Na}$  vs.  $\text{Ca}/\text{Na}$  spaces is drawn in Fig. 2. The main characteristic of waters draining evaporites is a depletion in  $\text{HCO}_3$  ion relative to Ca and Mg. Thus, the contribution of evaporites in large rivers results in a downward deviation of their representative point from the silicate–carbonate line in Fig. 2.

The relationships between  $^{87}\text{Sr}/^{86}\text{Sr}$  and  $\text{Sr}/\text{Na}$  are given on Fig. 4a. A similar picture would be obtained by plotting  $\text{Ca}/\text{Na}$  instead of  $\text{Sr}/\text{Na}$  because, as indicated by Fig. 4b, quite a good correlation exists between  $\text{Ca}/\text{Na}$  and  $\text{Sr}/\text{Na}$  molar ratios in large rivers. This correlation supports the mixing processes pointed out earlier between carbonates (high  $\text{Sr}/\text{Na}$  and  $\text{Ca}/\text{Na}$  ratios) and silicates or evaporites (low  $\text{Sr}/\text{Na}$ , low  $\text{Ca}/\text{Na}$  ratios). Water draining carbonates inherit the Sr isotopic composition of these rocks. The Sr isotopic composition of carbonates and its secular variation is now well documented (e.g., Burke et al., 1982). Over the Phanerozoic and Archean times the Sr isotopic composition of carbonates never exceeds 0.710 except when diagenetic recrystallisations occurred incorporating more radiogenic Sr. As a consequence the mean value of the Sr isotopic composition of the carbonate end member is fairly well defined. The same range of variation holds for evaporites, provided that most of the evaporites are marine. By contrast, for silicates, a much larger degree of scatter is expected because to a first order the Sr isotopic composition of silicates depends on their age. As

reported for example by Goldstein and Jacobsen (1987) on a global scale, or Allègre et al. (1996) in the Amazon and Congo river basins a correlation between Nd isotopic ratios in river particulates and Sr isotopic ratio is observed. Young magmatic provinces (with Nd model ages close to 0) have typical Sr isotopic ratios close to 0.705 while ancient provinces (for example, the Congo River Basin, Nd model age of 2 Ga) have Sr isotopic ratios close to 0.730. The non-uniformity of the isotopic composition of the silicate end member is also a characteristic of the Amazon drainage Basin, as seen by Gaillardet et al. (1997).

#### 4. Model and resolution

The following section is an attempt to apply the mixing model previously described for the Congo and Amazon river Basin (Négre et al., 1993; Gaillardet et al., 1997) to the set of large rivers selected here. The main purpose of the model is to calculate the contribution of silicate weathering to the present dissolved load of large rivers, on a global scale.

As suggested by Figs. 2 and 4, a limited number of major reservoirs is assumed to contribute to large river chemistry. These are rainwater, silicate, carbonate and evaporite derived waters. For a number of rivers strongly influenced by human activities, additional reservoirs have been introduced: agricultural effluent, domestic and industrial wastes and mining wastes.

A crucial step of the model is the determination of the river Cl concentration due to atmospheric inputs (cyclic Cl). Two complementary methods are used. When river basin monographs have been published (e.g., Indus, Congo, Amazon, Ganges rivers), the Cl concentration in the small rivers of the basin, whose geology supports that they do not drain any saline formation, are used to estimate the cyclic chloride concentration. The other method consists of multiplying the mean chloride concentration in rainwater by the evapo-transpiration factor. This factor is calculated for each river basin as the ratio of the water discharge over the average precipitation from the data of Meybeck and Ragu (1997).

The model is constituted of several mass budget equations which use elemental molar ratios and,

when available, Sr isotopic ratios. The general form of mixing equations (for  $X = \text{Cl, Ca, Mg, HCO}_3, \text{Sr}$ ) is:

$$\left(\frac{X}{\text{Na}}\right)_{\text{river}} = \sum_i \left(\frac{X}{\text{Na}}\right)_i \alpha_i(\text{Na})$$

where  $i$  = rainwater, silicate, carbonate, evaporite or human activities reservoirs. The  $\alpha_i$  are the mixing proportions of Na (the sum of the  $\alpha_i$  is equal to 1) in the different reservoirs from which the mixing proportions of the other elements are easily deduced. The equation for Sr isotopic composition is:

$$\left(\frac{{}^{87}\text{Sr}}{{}^{86}\text{Sr}}\right)_{\text{river}} \left(\frac{\text{Sr}}{\text{Na}}\right)_{\text{river}} = \sum_i \left(\frac{{}^{87}\text{Sr}}{{}^{86}\text{Sr}}\right)_i \left(\frac{\text{Sr}}{\text{Na}}\right)_i \alpha_i(\text{Na})$$

The main originality of this model is to be solved by an inversion method. Such a technique was used in the eighties by Allègre and Lewin (1989) for the chemical differentiation of the Earth. The main advantage of this technique is to take into account the errors that exist for each parameter used in the model. The error of a given parameter (e.g.,  $\text{Cl/Na}$  from evaporite) reflects the knowledge that we have on that parameter. The inversion procedure is particularly well suited for the aim of the present study, because as shown above, the chemical composition of the end members can only be known within a certain range of variability. For example, the 40% of relative uncertainty assigned to the Na-normalized ratios of the silicate end member reflects the natural variability we observe using the data on monolithological streams. The relative error on the alphas is 100%, because we, a priori, do not know what are the mixing proportions. The best known parameters are those that are deduced from measurements ( $\text{Cl}$  concentrations,  $X/\text{Na}$  river ratios).

The aim of the inversion procedure is to make all equations compatible (by adjusting the parameters chosen a priori to the model) and to calculate a new set of parameters for which errors have been improved (called 'a posteriori' parameters).

## 5. Results

The model presented above was applied to the 60 largest rivers and allowed to calculate the propor-

tions of Ca, Mg, Na, Cl,  $\text{HCO}_3$  and Sr (when data are available) derived from rain (cyclic salts) or from silicate, carbonate and evaporite weathering. The elements K and  $\text{SO}_4$  were not included into the mass budget model (due to our lack of knowledge of their global biogeochemical cycles) and their concentrations derived from silicate weathering were simply deduced from the concentrations of Na originating from silicate weathering using the typical ratios  $\text{K/Na} = 0.1$  and  $\text{SO}_4/\text{Na} = 0.2$  for silicate draining waters (Meybeck, 1986; Edmond et al., 1994).

Results (Figs. 5 and 6, Tables 2 and 3) will be discussed in terms of weathering rates (TDS in  $\text{mg l}^{-1}$ ,  $\text{t yr}^{-1}$  or  $\text{t km}^{-2} \text{ yr}^{-1}$ ), cationic weathering rates ( $\text{Na} + \text{K} + \text{Ca} + \text{Mg}$ ), and  $\text{CO}_2$  consumption rates (in  $\text{mol C yr}^{-1}$  or  $\text{t km}^{-2} \text{ yr}^{-1}$ ). Errors estimated on weathering rates are in general close to 30%, except for rivers dominated by one type of inputs (evaporation dominated rivers such as the Murray, carbonate dominated rivers such as the Changjiang) where errors propagated on the weathering rates of non-dominant inputs are more important.

Before examining the results, some important features and limitations of this mixing model must be kept in mind.

### 5.1. A number of singular rivers

For a number of rivers having singular features, it was not possible to strictly apply the model described above.

#### 5.1.1. Highly polluted rivers

European (Seine, Rhine, Weser, Elbe, Odra, Wisla, Nemanus, Danube and Po) and North American rivers (Mississippi and St. Lawrence) are highly polluted because they drain densely populated, industrialized and cultivated areas. As shown by Yang et al. (1996) for the St. Lawrence and by Flintrop et al. (1996) for the Rhine river, human activities can dominate the major element chemistry of such rivers. This is particularly evident for the Weser, Odra, Elbe and Wisla rivers (TDS up to  $2 \text{ g l}^{-1}$ ), which are dominated by the wastewater discharges of coal and salt mines of Northern Europe. Two main characteristics of very polluted rivers are TDS greater than  $500 \text{ mg l}^{-1}$  and  $\text{Cl/Na}$  molar ratios greater than that

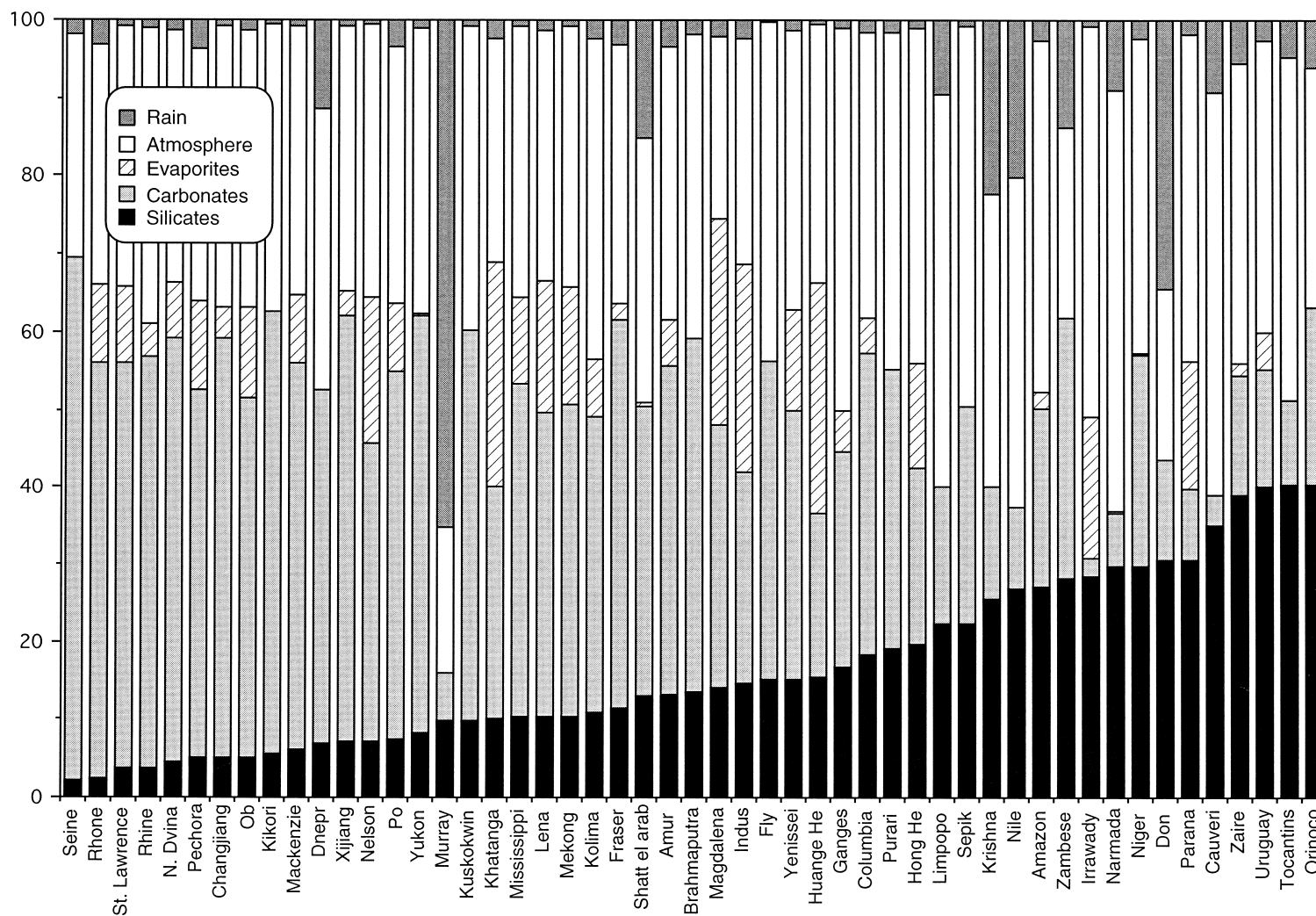


Fig. 5. Diagram showing for each river of this study, the contribution (as % of concentrations in  $\text{mg l}^{-1}$  of river water) of the different reservoirs. Rivers are ranked from left to right following the contribution of silicate weathering to total dissolved load. The atmospheric contribution corresponds to bicarbonate ions of atmospheric origin derived from carbonate and silicate weathering. The rain contribution corresponds principally to Na and Cl ions derived from seasalt dissolution.

Table 2

Chemical composition of the world average river water derived from silicate weathering and proportions of elements derived from silicate weathering with respect to the world average river water calculated using the largest rivers (this study). Comparison with estimates from previous authors

	World silicate average river ( $\mu\text{mol l}^{-1}$ )	This study (inverse method)	Meybeck (1987) <sup>a</sup>	Berner and Berner (1996) <sup>b</sup>
Na	98	41%	46%	22%
K	20	60%	82%	87%
Ca	34	10%	30%	18%
Mg	31	21%	48%	54%
HCO <sub>3</sub>	232	26%	35%	37%
SiO <sub>2</sub>	127	100%	90%	100%
Sr	0.18	31%		

<sup>a</sup>Calculated using data for small rivers draining monolithologies (Meybeck, 1986) and their outcrop proportions at the Earth surface. This apportionment does not take into account the atmospheric cyclic salts.

<sup>b</sup>Calculated using the data of Meybeck (1979) and a 'direct' method derived from that of Garrels and Mackenzie (1971).

of seasalts. In this paper, no attempt has been made to apply the model described above to the polluted rivers, as clearly, it would neglect the many anthropogenic contributions. To our knowledge, no study has tried to characterize the chemical attributes (if unique and constant through time and space) of the different anthropogenic sources to rivers. For the Seine river, an attempt has been made by Roy et al. (1999) to isolate the chemical features of the anthropogenic end members and to 'recalculate' the chemical composition of the pristine river. The influence of human activities is considerable on major element chemistry. As an example, only 25% of Na concentration in the modern Seine river is natural (cyclic and rock-derived). The results of Roy et al. (1999) were used. Finally, for the Rhine river, the chemical composition of the upper Rhine before the influence of Alsatian salt mines and the Rhur industrial and coal mining pollution (Buhl et al., 1991), was used to estimate the contribution of silicate weathering in this river. For the St. Lawrence and Mississippi rivers, the pre-industrial concentrations were taken from Meybeck (1979). For the Danube and the very polluted rivers of Northern Europe (Weser, Odra, Wisla), the contribution of rock weathering has not been calculated. Further extensive studies are necessary if we want to better understand the control of river chemistry in the most populated areas of the world.

### 5.1.2. Indian rivers

Two large rivers (the Godavari and Mahanadi rivers) and many smaller rivers of Southern and Central India are characterized by Cl/Na molar ratios greater than that of the ocean (Chakrapani and Subramanian, 1990; Ramanathan et al., 1994). Their chemical composition can thus not be simply explained by a mixing between seasalts (Cl/Na = 1.16) and halite (Cl/Na = 1) which are the main Cl sources in rivers. A first explanation of the Cl enrichment in Indian rivers is pollution, but this hypothesis has never been invoked by authors. The other and more probable cause of Cl enrichment is the presence, in the arid and semi-arid zones of India, of alkali soils in which minerals such as NaHCO<sub>3</sub>, Na<sub>2</sub>CO<sub>3</sub> and CaCO<sub>3</sub> precipitate. This sodification of soils (Chhabra, 1996) is a characteristic of areas exposed to repeated cycles of wetting and drying where the Na ions and the alkalinity are supplied by silicate weathering and transported by rivers or shallow groundwater. The impact of this process remains to be quantified at the scale of the largest rivers of India, but we propose that it could explain the Na depletion observed in the river chemistry of many waters of India. This process has also been suspected by Sarin et al. (1989) to play a role in the Indo-Gangetic plain. The Salween river is also enriched in Cl with respect to Na, and this could also reflect the influence of processes retaining Na in soils. All those

Table 3  
Results

Basins	Silicates				Carbonates		Evaporites		Total rock weathering		
	TDS <sub>sil</sub> (10 <sup>6</sup> t yr <sup>-1</sup> )	Cation sil (10 <sup>6</sup> t yr <sup>-1</sup> )	Ca + Mg sil (10 <sup>9</sup> mol yr <sup>-1</sup> )	CO <sub>2</sub> cons. (10 <sup>9</sup> mol yr <sup>-1</sup> )	TDS <sub>carb</sub> (10 <sup>6</sup> t yr <sup>-1</sup> )	CO <sub>2</sub> cons. (10 <sup>9</sup> mol yr <sup>-1</sup> )	TDS <sub>ev</sub> (10 <sup>6</sup> t yr <sup>-1</sup> )	CO <sub>2</sub> cons. (10 <sup>9</sup> mol yr <sup>-1</sup> )	10 <sup>6</sup> t yr <sup>-1</sup>	t km <sup>-2</sup> yr <sup>-1</sup>	CO <sub>2</sub> cons. (mol km <sup>-2</sup> yr <sup>-1</sup> )
Amazon	79.7	13.2	128	320	67.7	644	6	0	153	25	158
Changjiang	9.5	2.5	29	107	101	997	7	0	118	65	611
Mississippi	11.4	5.1	60	199	48.1	436	13	44	72	24	228
Irrawady	29.5	17.1	165	832	2.6	24	19	67	51	125	2250
Ganges	14.7	8.3	130	471	24.4	236	5	19	44	42	692
Yenisei	9.7	3.2	30	169	22.1	207	8	0	40	16	145
Mackenzie	3.2	1.6	19	61	26.7	242	5	11	35	19	176
St. Lawrence	1.9	0.8	9	28	26.5	251	5	17	33	33	290
Lena	5.4	1.7	19	86	20.5	187	9	0	35	14	110
Xijiang	4	0.7	9	24	30.2	283	2	6	36	82	715
Ob	2.4	1	11	57	21.9	217	5	26	30	10	100
Brahmaputra	6	1.5	19	87	20.5	199	0	0	27	46	493
Parana	13.9	3.4	69	263	4.2	51	7	31	26	9	124
Mekong	11.4	4.9	57	194	44.3	409	17	65	72	91	839
Congo–Zaire	15.6	3.1	34	201	6.2	51	1	0	22	6	68
Rhine	0.7	0.3	5	14	10.3	108	1	0	12	53	542
Yukon	2.7	0.9	13	29	17.3	164	0	0	20	24	227
Orinoco	10.5	2.5	29	76	6	55	0	0	16	15	119
Magdalena	3.6	0.5	7	15	8.7	82	7	33	19	81	554
Columbia	4.6	1.9	30	61	9.8	90	1	5	16	23	233
Indus	3.5	1.6	19	54	6.6	59	6	21	16	18	146
Don	6	4.4	55	48	2.6	23	0	0	9	20	169
Nelson	1.4	0.9	10	43	7.2	65	4	15	12	11	109
N. Dvina	0.7	0.3	4	9	8	69	1	3	10	28	232
Amur	2.2	1.1	13	33	7.2	64	1	3	10	6	54
Huanghe	2.6	1.6	19	62	3.5	30	5	17	11	15	144

Rhone	0.4	0.1	1.4	4.7	8.4	74	2	3	10	109	856
Shatt el Arab	2	1.2	14	37	5.7	49	0	0	8	14	157
Hong He	3.3	1.5	17	82	3.8	36	2	10	9	78	1062
Po	1	0.6	7	16	6.6	58	1	4	9	126	1119
Fly	2.4	0.9	17	49	6.7	66	0	0	9	149	1884
Tocantins	5.7	1	11	87	1.6	15	0	0	7	10	135
Dnepr	0.9	0.5	6	21	5.9	55	0	0	7	13	150
Sepik	3	1.2	22	72	3.8	36	0	0	7	87	1378
Nile	2.9	1.8	21	64	1.2	11	0	0	4	1	26
Narmada	3.5	2.3	29	95	0.8	9.5	0	0	4	43	1026
Murray Darling	1	0.6	9	25	0.6	5.6	0	0	2	2	29
Purari	2	0.7	12	37	3.8	37	0	0	6	189	2428
Fraser	1.1	0.3	4	9.4	4.7	42	0	1	6	27	238
Kolima	0.9	0.3	3	29	3.2	27	1	2	5	7	88
Krishna	2.1	1.4	18	41	1.2	11	0	0	3	13	197
Pechora	0.4	0.1	2	5.8	3.8	37	1	4	5	16	144
Niger	2.7	0.4	4.2	35.5	2.5	25	0	0	5	4	50
Uruguay	3.2	0.9	18	38.9	1.2	11	0	1	5	20	212
Kuskokwin	0.8	0.2	4	12.3	3.9	38	0	0	5	38	408
Cauveri	2.4	1.5	18	56	0.3	2.4	0	0	3	31	665
Zambese	2.2	0.4	4.5	9.2	2.7	22	0	0	5	4	24
Khatanga	0.8	0.4	4.2	15.4	2.3	21	2	9	5	15	126
Seine	0.1	0.06	0.5	1	2.6	17	0	0	3	34	226
Kikori	0.4	0.1	1.1	2.5	4.1	41	0	0	4	338	3265
Limpopo	1.4	0.7	8	42.4	1.1	9.5	0	0	3	6	118
World average	550	200	2500	8700	1290	12 300	290	900	2131	24	246

TDS: total dissolved solids. The subscripts sil, carb, and ev denote, respectively silicates, carbonates and evaporites.

Cation sil: Na + K + Ca + Mg concentrations derived from silicate weathering.

Ca + Mg sil: Ca + Mg concentrations derived from silicate weathering.

CO<sub>2</sub> cons.: flux of atmospheric CO<sub>2</sub> fixed up by weathering reactions.

Weathering fluxes classified by lithologies and total weathering fluxes.

rivers that have Cl/Na ratios greater than that of seawater cannot be modeled by the method described earlier. However, we are aware that in rivers having Cl/Na lower than that of seawater (such as the Cauvery river in South India and other semi arid areas in the world) the non-existence of such secondary processes (tending to increase the Cl/Na ratio) cannot be ruled out. The existence of such secondary processes which modify the chemistry of the soil solution is a severe limitation to the approach developed in this paper.

### 5.1.3. Siberian rivers

The last group of rivers having Cl/Na ratios greater than seawater are rivers from Siberia. This concerns the Lena river, its tributaries (Gordeev and Sidorov, 1993) and the Yenisei river. These rivers are clearly not affected by pollution and like for Indian rivers, a source of high Cl/Na ratio is necessary to explain the river chemistry. Saline formations (halite) are present within the drainage area but cannot explain Cl/Na ratios greater than 1. As reported by Gordeev and Sidorov (1993), the most probable explanation for their enrichment in Cl is the contribution of very saline groundwater. The existence of Na–Ca–Cl brines having Cl/Na ratios close to 3 in granitic areas have been documented by many studies (e.g., Frape and Fritz, 1981). In Siberian brines, these authors report Cl–Ca brines having Cl/Na ratios up to 10 and Ca/Na ratios up to 8. In the present study the results for silicate, carbonate and salt contribution in Siberian rivers were obtained by assuming that Cl is mainly derived from saline groundwater having  $\text{Cl/Na} = 3$ ,  $\text{Ca/Na} = 1$ ,  $\text{Mg/Na} = 0.05$  and  $\text{HCO}_3^-/\text{Na} = 0.001$ . If some Cl is assumed to be derived from halite ( $\text{Cl/Na} = 1$ ), then the proportions of silicate weathering decrease. The total dissolved solids from silicate weathering calculated for the Lena and Yenisei rivers are thus the maximum ones. Clearly, more intensive studies on the provenance of dissolved salts in the large rivers of Siberia are necessary.

### 5.2. Sources of solutes

The contribution of rock weathering (silicate, carbonate and saline rocks), rain and atmosphere is shown in Fig. 5 for each river selected in this study.

Rivers are ranked by decreasing silicate weathering contribution.

- The participation of silicate weathering to the dissolved load of rivers never exceeds 40%. The rivers most influenced by silicate weathering are the Orinoco, Tocantins, Uruguay, Zaire, Cauveri (India) and Parana. The rivers least influenced by silicate weathering are those draining large sedimentary basins such as the Seine, Rhine, N. Dvina and Pechora rivers.

- All the largest rivers of the world are, to a greater or lesser extent, influenced by carbonate dissolution. Carbonate dissolution is particularly important for the Kikori, Xijiang and Changjiang rivers in which more than 50% of the TDS originates from carbonate weathering. By contrast the Irrawady, Cauveri, Murray Darling, Narmada, Parana and Tocantins rivers have less than 10% of their dissolved loads derived from carbonate dissolution.

- The dissolution of evaporites appears to play a major role in the Huanghe, Khatanga, Indus and Magdalena rivers in which it represents more than 20%. More than 20 large rivers are not influenced by evaporite dissolution. (e.g., Cauveri, Fly, Niger).

- For most large rivers, rain inputs are almost insignificant (less than 5%) except for those rivers most influenced by evaporation. An example of such a river is the Murray Darling in which 70% of solutes originates from rainwater. This result is in agreement with the conclusions of Herczeg et al. (1993).

- Finally the contribution of atmospheric  $\text{CO}_2$  via carbonate and silicate weathering fluctuates from 20% (Murray Darling river) to about 40% in the Narmada and Cauveri rivers.

On a global scale, the source of solutes in a average world river ( $\text{TDS} = 100 \text{ mg l}^{-1}$ ) can be separated into  $15 \text{ mg l}^{-1}$  of solutes derived from silicate weathering,  $35 \text{ mg l}^{-1}$  derived from carbonate weathering,  $8 \text{ mg l}^{-1}$  derived from evaporite dissolution,  $3 \text{ mg l}^{-1}$  derived from rainwater and  $37 \text{ mg l}^{-1}$  of solutes constituting of  $\text{HCO}_3^-$  derived from atmospheric  $\text{CO}_2$  consumed by carbonate and silicate weathering. The chemical composition of the average world river water, only derived from silicate weathering, is given in Table 2 with the proportions of each element originating from silicate weathering. The proportions of Berner and Berner (1996) were



determined following the approach initiated by Garrels and Mackenzie (1971) using the river data set of Meybeck (1979) and appear to be somewhat different from those determined here. The proportions of Meybeck (1987) were determined using water analysis of rivers draining major rock type and their outcrop proportions. They also differ from the results of this study in the sense that more Ca, Mg, and  $\text{HCO}_3^-$  ions are found to be derived from silicate weathering than in our study.

In order to test the sensitivity of the method to the choice of a priori Na-normalized ratios of the silicate end member, we calculated the proportions of elements originating from silicate weathering by assuming that the silicate-draining waters have higher Na-normalized ratios:  $\text{Ca}/\text{Na} = 1 \pm 0.4$ ,  $\text{Mg}/\text{Na} = 0.6 \pm 0.2$ ,  $\text{HCO}_3^-/\text{Na} = 3 \pm 1$  and  $\text{Sr}/\text{Na} = 5 \pm 2 \times 10^{-3}$ . The uncertainties calculated on the percentage of elements derived from each source are greater using this set of a priori parameter than that used above. Within errors, the proportions of Na and K derived from silicates remain unchanged, while the Ca, Mg,  $\text{HCO}_3^-$  and Sr proportions increase to 16%, 30%, 31% and 34%, respectively. These proportions are still lower than that found by previous studies.

### 5.3. Weathering rates

The weathering fluxes, calculated for each river and for the average world river, are shown in Table 3. Because for some rivers (Amazon, Zaire, Orinoco, Niger, Zambese), dissolved silica represents a dominant part of the TDS issued from silicate weathering, the cationic weathering rates (either total:  $\text{Na} + \text{K} + \text{Ca} + \text{Mg}$  or derived from Ca–Mg silicates:  $\text{Ca} + \text{Mg}$ ) are also given. A good global correlation is observed between cationic silicate weathering fluxes and total silicate weathering fluxes (Fig. 6a). Silica rich rivers deviate somewhat from this global trend (Amazon, Zaire, Orinoco, Niger, Zambese).

Silicate weathering fluxes range from  $80 \times 10^6 \text{ t yr}^{-1}$  to  $0.1 \times 10^6 \text{ t yr}^{-1}$  (Seine river). The rivers having the highest silicate weathering fluxes are the Amazon ( $80 \times 10^6 \text{ t yr}^{-1}$ ), the Irrawady ( $30 \times 10^6 \text{ t yr}^{-1}$ ) and the Zaire ( $16 \times 10^6 \text{ t yr}^{-1}$ ). On a global scale  $300 \times 10^6 \text{ t yr}^{-1}$  of dissolved solids derived from silicate weathering are transported into the ocean by the 60 largest rivers. For comparison,

$640 \times 10^6 \text{ t yr}^{-1}$  of dissolved substances originating from carbonate weathering and  $144 \times 10^6 \text{ t yr}^{-1}$  for evaporites are transported to the sea. Thus, the total flux of dissolved material inherited from chemical weathering is  $1080 \times 10^6 \text{ t yr}^{-1}$ . Given that about 51% of the continental runoff is represented by the rivers used here, and assuming that the world average river composition calculated on the basis of the 60 largest rivers is a good estimate of the whole surface area of external drainage, we come to the value of about  $2130 \times 10^6 \text{ t yr}^{-1}$  of dissolved material originating from rock weathering. The flux of material originating from silicate weathering is about  $550 \times 10^6 \text{ t yr}^{-1}$ , or 26% of the total flux.

However, it is important to note that the reliability of these results depends on the assumption that the world river average composition calculated here is a good estimate of what would be calculated using all the rivers on Earth. This extrapolation may not be true, especially because the average river water calculated here does not take into account oceanic islands (such as Iceland or Hawaii) and volcanic arc areas (as Kamtchatka and Philippines arcs) which are partly or entirely constituted of basaltic rocks. According to the results of Louvat (1997), basalts from oceanic and arc islands weather at very high rates of about  $100 \text{ t km}^{-2} \text{ yr}^{-1}$ . Estimating the surface area of oceanic islands and volcanic arcs to  $1.5 \times 10^6 \text{ km}^2$ , we obtain a flux of about  $150 \times 10^6 \text{ t yr}^{-1}$ , or 25% of the flux derived from continental silicates calculated above. There is however a large uncertainty on this additional flux because the weathering rate of  $100 \text{ t km}^{-2} \text{ yr}^{-1}$  is an average calculated using rivers of Iceland, Azores, Java and Reunion Island. The flux of silicate weathering given above is thus a minimum value and it needs to be improved by incorporating more rivers draining the volcanic provinces of arc and islands.

For comparison, the total sediment discharge (mainly derived from the mechanical erosion of silicates) to the ocean is estimated by Milliman and Syvitski (1992) to be  $20\,000 \times 10^6 \text{ t yr}^{-1}$ . The weathering processes of silicates are thus dominated by mechanical erosion and can be characterized by a global mechanical to chemical weathering ratio of 36. The total silicate denudation (mechanical and chemical) is thus  $20\,550 \times 10^6 \text{ t yr}^{-1}$  or, using a mean rock density of 2.7, 8.6 cm per thousand years.

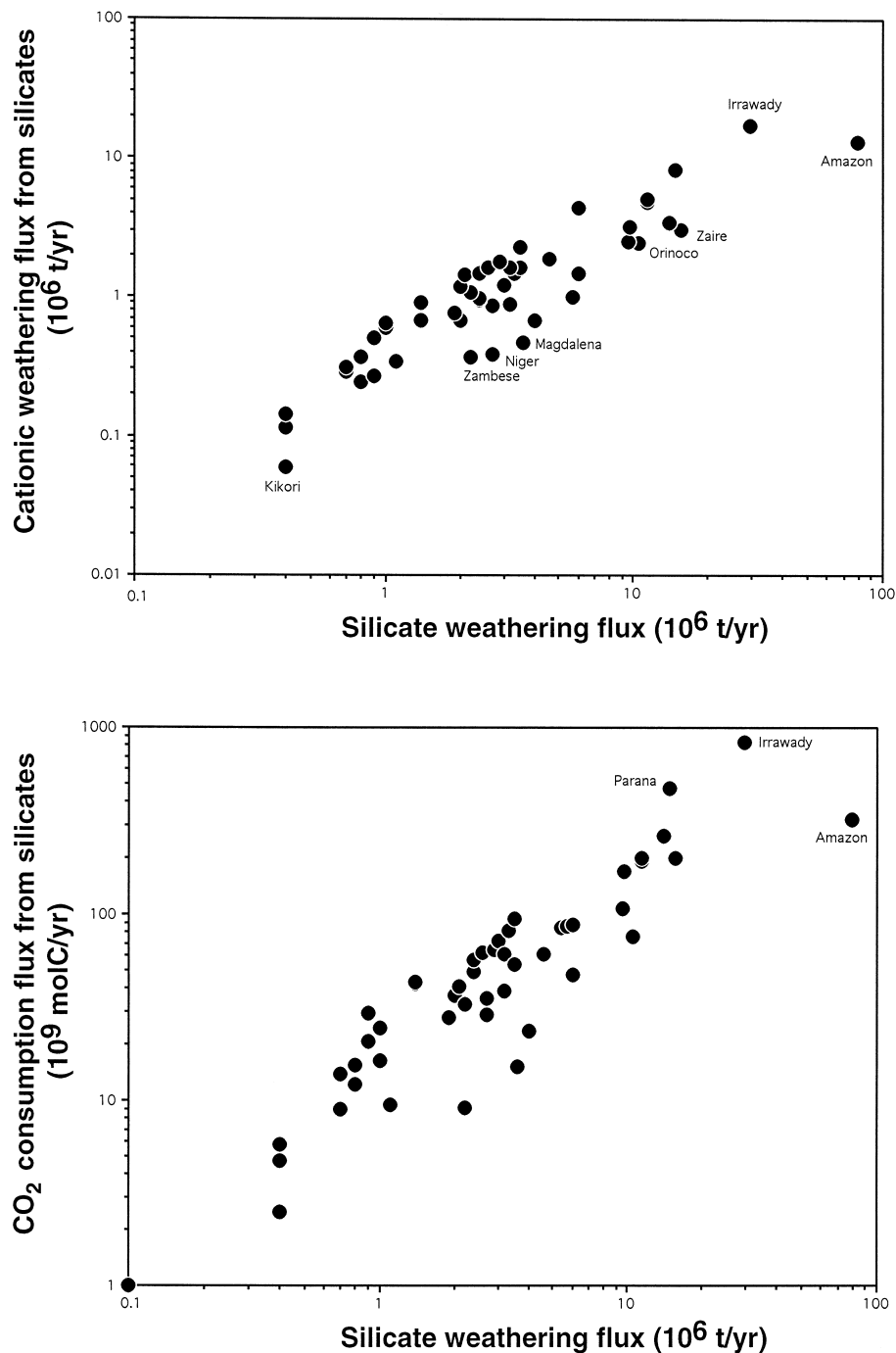


Fig. 6. Relationships between the fluxes of material derived from the chemical weathering of silicates and (a) the fluxes of cations derived from silicate weathering and (b) the flux of CO<sub>2</sub> removed from the atmosphere by the weathering of aluminosilicates. The deviation of rivers such Amazon, Zaire, Orinoco from the main trend is due to their high silica concentration relative to cations.

The total world average chemical denudation flux, calculated from the present study, is  $24 \text{ t km}^{-2} \text{ yr}^{-1}$ . This is the rate at which silicates, carbonates and evaporites are being removed from the continents. The maximum rates are observed for the rivers of Papua N.G. and the river Irrawady. These rates do not take into accounts the weathering of oceanic island basalts which have an average chemical denudation of  $100 \text{ t km}^{-2} \text{ yr}^{-1}$ . This world average rate is in good agreement with those reported by Meybeck (1979) and Berner and Berner (1996), respectively, 26 and  $21 \text{ t km}^{-2} \text{ yr}^{-1}$ .

#### 5.4. $\text{CO}_2$ consumption rates

A good linear correlation (Fig. 6b) is observed between  $\text{CO}_2$  consumption fluxes and silicate weathering fluxes (also between specific fluxes). Thus, the observations pointed out above for silicate weathering rates also hold for  $\text{CO}_2$  consumption rates.

The influence of rock weathering on atmospheric  $\text{CO}_2$  must be considered differently with respect to time frame. Following the approach of Berner et al. (1983), in less than 100 000 years (the time required by rivers to transport dissolved C in the oceans), weathering of all lithologies is important for the consumption of  $\text{CO}_2$  from the atmosphere. With respect to million years, C supplied from the land by carbonate weathering is removed from the sea by calcite precipitation and soon returned to the atmosphere. Carbonate weathering has thus no effect on atmospheric  $\text{CO}_2$ . The only significant reactions are weathering reactions of Ca and Mg silicates on continents transforming  $\text{CO}_2$  from the atmosphere to  $\text{HCO}_3^-$  in rivers and leading to precipitation of carbonate minerals in the ocean. The control of atmospheric  $\text{CO}_2$  by the weathering of Na and K silicate minerals on land is less obvious as alkalis are involved in 'reverse weathering' reactions in seawater, leading to the formation of Na and K silicates and converting  $\text{HCO}_3^-$  to  $\text{CO}_2$  that returns to the atmosphere. According to these considerations, we will give separately the  $\text{CO}_2$  consumption rates from carbonate weathering, Ca and Mg silicate weathering and total silicate weathering.

On a global scale, the consumption of  $\text{CO}_2$  by rock weathering is  $8700 \times 10^9 \text{ mol yr}^{-1}$  ( $0.104 \text{ Gt C yr}^{-1}$ ) for silicate weathering and  $12300 \times 10^9 \text{ mol}$

$\text{yr}^{-1}$  ( $0.148 \text{ Gt C yr}^{-1}$ ) for carbonate weathering (Table 3). The weathering of Ca and Mg aluminosilicates consumes approximately  $5000 \times 10^9 \text{ mol yr}^{-1}$  ( $0.060 \text{ Gt C yr}^{-1}$ ) according to Table 3 (60% of total flux derived from silicate weathering). Thus, we can estimate that the global flux of  $\text{CO}_2$  consumption by rock weathering is  $0.252 \text{ Gt C yr}^{-1}$ , 40% of which is due to the weathering of Na, K, Ca and Mg silicates.

As discussed above, in order to test the sensitivity of the flux calculations to the choice of a priori Na-normalized ratios for the silicate end member, we calculated the fluxes of consumed  $\text{CO}_2$  under the hypothesis that the silicate-draining waters have higher Na-normalized ratios ( $\text{Ca/Na} = 1 \pm 0.4$ ,  $\text{Mg/Na} = 0.6 \pm 0.2$ ,  $\text{HCO}_3^-/\text{Na} = 3 \pm 1$  and  $\text{Sr/Na} = 5 \pm 2 \times 10^{-3}$ ). The so-calculated flux of  $\text{CO}_2$  consumption increases to about  $10600 \times 10^9 \text{ mol C yr}^{-1}$ , 20% higher than the flux determined using the set of 'low' Na-normalized values for the silicate end member. Within the precision assigned to this flux ( $\pm 30\%$ ), we do not consider it drastically different from that previously estimated.

For the same reasons drawn for chemical weathering fluxes, this value of  $\text{CO}_2$  consumption does not include the  $\text{CO}_2$  consumed during weathering of basalts from volcanic arcs and volcanic islands. According to the results of Louvat (1997), the specific  $\text{CO}_2$  consumption rates due to basalt weathering range from  $0.3$  to  $4 \times 10^6 \text{ mol C km}^{-2} \text{ yr}^{-1}$ , with an average value of  $2 \times 10^6 \text{ mol C km}^{-2} \text{ yr}^{-1}$ . About 70% of this flux can be attributed to the weathering of Ca + Mg aluminosilicates. At a global scale, we thus calculate that the weathering of these young volcanic rocks consumes  $3000 \times 10^9 \text{ mol C yr}^{-1}$  ( $0.036 \text{ Gt C yr}^{-1}$ ) and that about  $0.025 \text{ Gt C yr}^{-1}$  is consumed by the weathering of Ca and Mg aluminosilicates. If these estimates are correct, the contribution of volcanic islands and arcs to global  $\text{CO}_2$  consumption by rock weathering appear thus to be more than 30% of the  $\text{CO}_2$  consumption flux of continents. Again, more local studies are necessary to refine this proposition.

We finally propose that the present-day  $\text{CO}_2$  flux consumed by chemical weathering of silicates (continental and volcanic rocks) should approach  $0.140$  and  $0.085 \text{ Gt C yr}^{-1}$  if we only consider the weathering of Ca–Mg silicates. Adding the flux derived from carbonate weathering, the total flux of atmo-

Table 4

CO<sub>2</sub> consumption fluxes by carbonate and silicate weathering in mol C yr<sup>-1</sup>

	This study	Amiotte-Suchet and Probst (1995)	Meybeck (1987)	Berner et al. (1983)	Holland (1978)
Carbonate weathering	$12.3 \times 10^{12}$		$12 \times 10^{12}$	$11.8 \times 10^{12}$	$14 \times 10^{12}$
Silicate weathering	$11.7 \times 10^{12a}$		$12.6 \times 10^{12}$	$11.5 \times 10^{12b}$	$23 \times 10^{12}$
Total	$24 \times 10^{12}$		$24.6 \times 10^{12}$	$23.3 \times 10^{12b}$	$37 \times 10^{12}$
	0.288 Gt C yr <sup>-1</sup>	0.26 Gt C yr <sup>-1</sup>	0.29 Gt C yr <sup>-1</sup>	0.28 Gt C yr <sup>-1</sup>	0.44 Gt C yr <sup>-1</sup>

<sup>a</sup>Includes  $8.7 \times 10^{12}$  mol C yr<sup>-1</sup> derived from continental rocks weathering +  $3 \times 10^{12}$  mol C yr<sup>-1</sup> derived from weathering of volcanic rocks from oceanic islands and volcanic arcs.

<sup>b</sup>These fluxes do not include the contribution of Na and K silicates weathering.

spheric CO<sub>2</sub> consumed by rock weathering is 0.288 Gt C yr<sup>-1</sup>. Our value for the global flux of CO<sub>2</sub> consumption by rock weathering is compared to other previous estimates by rock weathering in Table 4. Our value is very close to that of Meybeck (1987), but is 30% lower than that of Holland (1978). When comparing with Berner et al. (1983), it must be kept in mind that his estimation does not take into account the weathering of Na and K silicates. The calculation of the similar flux (for Ca and Mg silicates weathering) using our data gives  $7100 \times 10^9$  mol yr<sup>-1</sup> (0.085 Gt C yr<sup>-1</sup>), 40% lower than that estimated by Berner et al. (1983).

Finally, it is interesting to compare rock weathering and organic weathering fluxes. Organic weathering corresponds to the net loss of organic matter from the ecosystems to rivers in a dissolved (DOC) or solid (POC) form. The flux of organic carbon transported annually to the ocean by rivers is 0.38 Gt C yr<sup>-1</sup>, 0.17 Gt C yr<sup>-1</sup> of which are in a particulate form (Ludwig et al., 1996). The total flux of organic carbon is thus 30% higher than the flux derived from chemical weathering of rocks and about four times the flux of C derived from Ca and Mg silicate weathering. At a multimillion-year time scale, if we consider that Ca and Mg silicate weathering reactions exert the dominant control on CO<sub>2</sub> consumption, and that the majority of organic carbon transported in rivers is buried in oceanic sediments, then it appears that silicate weathering is four times less efficient than organic weathering. This conclusion is consistent with that of France-Lanord and Derry (1997), who showed that the Neogene CO<sub>2</sub> consumption resulting from the net burial of organic

carbon in the Bengal Fan was 2–3 times than that derived from the weathering of Himalayan silicates.

## 6. Global control of weathering rates and CO<sub>2</sub> consumption

Many variables, geologic, climatic or topographic may potentially control the chemical denudation of the continents. The search for causal links between weathering rates and morphometric or climatic variables is complicated by the strong statistical associations between these variables (e.g., runoff and temperature, runoff and relief).

### 6.1. Lithology

The first factor to play an important role, if not a dominant one, on chemical denudation, is rock type. This was clearly pointed out early by Garrels and Mackenzie (1971), confirmed and quantified by Meybeck (1987) and more recently by Amiotte-Suchet and Probst (1993), Bluth and Kump (1994) and Edmond et al. (1996). Based on the study of small rivers draining only one type of rock, Meybeck (1987) has proposed that the relative chemical weathering rates of continents range from 1 for granite and gneiss to 12 for limestones and 80 for saltrocks.

One major advantage of the present study is that, for each large river, the contribution of carbonate and evaporite dissolution to the total dissolved load has been estimated. This enables us to address the

comparison and control of silicate chemical weathering rates on a global scale.

Nevertheless, it is very important to keep in mind that the specific silicate weathering rates, expressed as tonnes of dissolved solids from silicate weathering washed off per square kilometer of land per unit of time (product of TDS from silicates and river runoff), are underestimated because the surface area of silicate rocks is lower than that of the total surface area. This bias toward lower values of silicate chemical weathering is maximum when carbonates dominate the river chemistry (e.g., Changjiang, Xijiang). To avoid this problem, two approaches can be followed.

- The first one will be to estimate the surface area of silicate rock outcrops using geological maps, and then to calculate silicate weathering rates using the surface area of silicate rocks only. We believe that this is not the best approach for many reasons. Some lithologies may be hidden by superficial formations or thick soils and may not appear on geological maps. Within the Congo basin, limestones exist (as can be seen in river chemistry, cf. Négrel et al., 1993; Probst et al., 1994), but are not reported on geological maps because they lie under a lateritic cover. In sedimentary basins, carbonate series are never constituted of pure limestones and contain detrital silicates, whose ‘true’ surface area cannot be estimated from geological maps.

- The second approach consists of weighting each specific silicate denudation rate (calculated using the total surface area) by an index of silicate dissolution. We chose the ratio of  $\text{HCO}_3^-$  concentration derived from silicate weathering over  $\text{HCO}_3^-$  concentration from rock weathering as an index ( $\%H_{\text{sil}}$ ) of carbonate–silicate dissolution. A value of  $\%H_{\text{sil}} = 1$  means that bedrocks are essentially silicates. Normalized weathering rates are calculated as follows:

$$\text{normalized specific rate} = \left( \frac{\text{TDS}_{\text{sil}} \cdot \text{Runoff}}{\%H_{\text{sil}}} \right)$$

The so-normalized weathering rates do not have any physical sense and only relative variations are of interest. This new set of weathering rates, normalized to the value for the Amazon river, is given in Table 5. These weathering rates are thus expressed in number of times the silicate weathering rate of sili-

cates in the Amazon basin. The same formalism can be applied to the specific fluxes of cations ( $\text{Na} + \text{K} + \text{Ca} + \text{Mg}$ ) inherited from silicate weathering, and to the  $\text{CO}_2$  consumption rates from silicate weathering.

For the Po and Rhone rivers the true values are probably lower, because the cations from these rivers were not corrected for pollution (agriculture, industry and domestic waste). In addition, for rivers whose chemistry is dominated by carbonate weathering, i.e., having proportions of  $\text{HCO}_3^-$  from silicate over total  $\text{HCO}_3^-$  ( $\%H_{\text{sil}}$ ) close to 0.05 (Xijiang, Changjiang, St. Lawrence, Kikori, Seine, Rhone, Rhine, N. Dvina, Magdalena and Yukon), an important error is propagated on the relative chemical weathering rates of Table 5 ( $\pm 2$  for the Xijiang) and must be kept in mind. The highest cation weathering rates are observed for the Purari (5) and Fly (3.5) and the rivers from the Himalayas (Irrawady, Mekong, Brahmaputra). The highest chemical weathering rates are obtained for the Purari (11), Fly (9), Irrawady (7), Mekong (5), Sepik (5). Conversely, the rivers having the lowest total and cationic weathering rates are the Murray, Nile (0.1), Limpopo, Kolima, Niger and Zaire (0.16). The whole range of silicate weathering rates span two orders of magnitude.

## 6.2. Climate: runoff and temperature

A good linear log–log correlation is observed between runoff (water discharge/surface area) and weathering rates (Fig. 7a). In Fig. 7, the small rivers draining only volcanics at Reunion Island, Azores, Iceland and Java (Louvrat, 1997) are plotted for comparison. They are in excellent agreement with the correlation of large rivers and fall near the basalt-dominated rivers of Papua N.G. This correlation would confirm, on a global scale, the classical view that runoff has a strong control on chemical weathering rates of silicates. Many studies of silicate weathering in small rivers (e.g., Dunne, 1978; Bluth and Kump, 1994) have reported similar log–log correlation between runoff and weathering rates.

The important question of the inevitability of such log–log correlation must however be raised. Weathering rate vs. runoff diagrams simply consist of plots of  $\text{TDS} \times \text{Runoff}$  vs. Runoff. Using logarithmic co-

Table 5  
Relative chemical and physical weathering rates of silicates

	Relative chemical weathering rates	Relative cationic weathering rates	Relative physical weathering rates
Amazon	1	1	1
Changjiang	2.6	4.2	8.8
Mississippi	0.54	1.5	0.66
Irrawady	2.1	7.3	1.2
Ganges	0.72	2.5	1.8
Yenisei	0.33	0.65	0.03
MacKenzie	0.41	1.3	0.35
St. Lawrence	0.91	2.3	0.13
Lena	0.29	0.6	0.06
Xijiang	5.8	5.9	6.9
Ob	0.19	0.46	0.08
Brahmaputra	1.5	2.2	8.7
Parana	0.19	0.29	0.07
Mekong	2	5.2	1.8
Congo–Zaire	0.16	0.19	0.02
Rhine	1.4	3.3	0.42
Yukon	1	1.9	1.4
Orinoco	0.59	0.83	0.56
Magdalena	5.4	4.3	22
Columbia	0.7	1.7	0.15
Indus	0.35	0.98	1.7
Don	0.71	3.2	0.02
Nelson	0.13	0.53	
N. Dvina	0.8	2.3	0.38
Amur	0.15	0.44	0.11
Huanghe	0.19	0.74	5.5
Rhone	3.3	6.1	16
Shatt el arab	0.34	1.2	1.2
Hong He	1.4	3.8	3.6
Po	3	11	3.1
Fly	3.7	8.8	12
Tocantins	0.26	0.28	0.23
Dnepr	0.28	0.99	0.05
Sepik	1.9	4.7	0.35
Nile	0.1	0.36	0.09
Narmada	1.05	4.2	2.4
Murray	0.03	0.13	0.07
Purari	5	11	13
Fraser	1.3	2.4	1.5
Kolima	0.1	0.18	0.12
Krishna	0.31	1.3	0.63
Pechora	0.45	0.97	0.49
Niger	0.14	0.12	0.13
Uruguay	0.54	0.89	0.12
Kuskokwin	1.1	2.2	0.68
Cauveri	0.76	2.8	
Zambese	0.25	0.25	0.15
Khatanga	0.24	0.68	0.03
Seine	0.83	1.3	0.41

Table 5 (continued)

	Relative chemical weathering rates	Relative cationic weathering rates	Relative physical weathering rates
Kikori	26	24	
Limpopo	0.12	0.34	0.18

All weathering rates are normalized to that of the Amazon river. For the Xijiang, Changjiang, St. Lawrence, Kikori, Seine, Rhone, Rhine, N. Dvina, Magdalena and Yukon rivers, whose river chemistry is dominated by carbonate dissolution, an important error (ca. 50%) is propagated on the weathering rates (see text).

ordinates, a linear correlation with a slope close to 1 simply means that TDS values (in  $\text{mg l}^{-1}$ ) fluctuate much less than runoff values from one river to another. While impressive, log–log correlations of weathering rates vs. runoff probably have little physical sense, simply showing that the amount of solutes released by weathering is more or less constant with runoff. As shown in Fig. 7a, the slope of the correlation obtained for the large rivers of this study is not significantly different from 1, showing the relative constancy of normalized TDS values of silicates from one large river to another. Nevertheless, by itself, this constancy shows that with increasing runoff, the intensity of chemical weathering increases and counterbalances dilution. Authors (e.g., Berner, 1994) have used global relationships between concentrations and runoff represented by the expression  $C = kR^{-r}$  with  $r < 1$  ( $r = 0.35$  for Berner, 1994). Here, scatterplots of normalized total dissolved load ( $\text{TDS}_{\text{sil}}/\%H_{\text{sil}}$ ) or normalized cationic load ( $\text{Na} + \text{K} + \text{Ca} + \text{Mg}$ ) derived from silicate weathering vs. runoff do not show any general relation for large rivers. The large degree of scatter that is apparent from these plots or on the correlation of Fig. 7a (of about one order of magnitude for runoff values between 100 and 1000  $\text{mm yr}^{-1}$ ), tends to show that runoff is not a parameter of prime importance for the prediction of silicate weathering rates from large rivers. Concerning the role of temperature, it is particularly interesting to note that the Kuskokwin river (Alaska), while having about the same runoff values than Zaire river, has 10 times higher silicate weathering rates (about the same factor is obtained for cation weathering fluxes). The

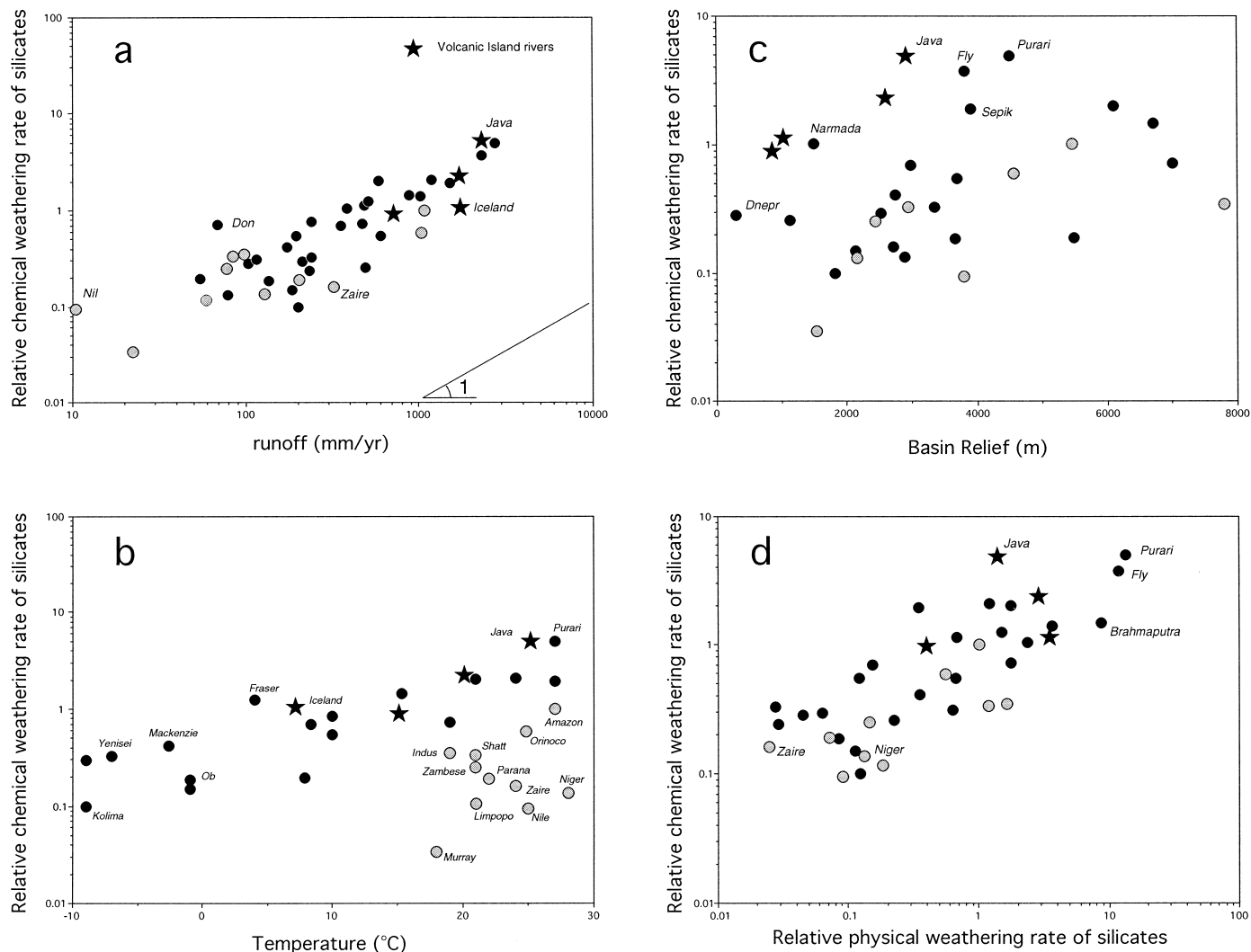


Fig. 7. Scatter plots of relative chemical weathering rates of silicates (see text for definition) calculated for largest rivers vs. various potentially controlling variables. The large rivers dominated by carbonate dissolution (Xijiang, Changjiang, St. Lawrence, Kikori, Seine, Rhone, Rhine, N. Dvina, Magdalena and Yukon) have not been plotted on these diagrams because the error propagated on their silicate weathering rates is too large. The results for small rivers draining volcanic islands from Louvat (1997) are plotted for comparison. The shaded circles correspond to the rivers deviating from the main trend of the chemical silicate weathering vs. temperature diagram.

relationship between chemical silicate weathering rates and temperature is explored on Fig. 7b. Temperatures are taken from Meybeck and Ragu (1997). It must be kept in mind that such values are average values and can hide large variations (e.g., from 0°C to 25°C for the Amazon river basin). On a global scale, there is no general correlation of weathering rates (total or cationic) with temperature. It is however interesting to note that, if we exclude from the data set a number of rivers (Indus, Shatt, Murray, Nile, Niger, Zaire, Zambese, Limpopo, Parana, Orinoco, Amazon), for which chemical weathering rates are relatively low given their average temperature, then a reasonable positive correlation appears between weathering rates and temperature. A large scatter characterizes this correlation with the same range of variation for a given runoff as the total range of variation between arctic and tropical regions. Along this 'line', weathering rates increase about 5 times every 5°C. The rivers characterized by high temperatures and low chemical weathering rates have been plotted distinctively from others on Fig. 7. For half of them, the relatively low weathering rates can be explained by excessively low runoff values ( $< 100 \text{ mm yr}^{-1}$  for the Nile, Murray, Zambese, Limpopo, Shatt and Indus rivers). A plot of temperature vs. runoff values clearly shows that these two parameters are linearly correlated except for these peculiar rivers that deviate from the main trend toward the high temperature and low runoff field. This 'runoff effect' explains the low chemical weathering rates of the Nile, Murray, Zambese, Shatt, Limpopo and Indus rivers but cannot be invoked for the other rivers (Amazon, Zaire, Orinoco, Zaire, Parana and Niger) for which weathering rates of silicates are low in spite of optimum climatic conditions. The large rivers of the humid intertropical zone are thus not characterized by the highest chemical weathering rates of silicates. From this study, we conclude that temperature and runoff are not overriding parameters controlling chemical weathering rates of silicates deduced from large river chemistry. This conclusion contrasts with that of White and Blum (1995) based on the study of experimental watersheds underlain by granitoid rocks or with results from experimental studies of silicate dissolution (Brady and Carroll, 1994) both giving to temperature and precipitation the dominant role in the control of

weathering rates and ascribing to tropical regions a major importance in global weathering.

### 6.3. Relief parameters

We tested the influence of many morphometric parameters (taken from Summerfield and Hulton, 1994 and Pinet and Souriau, 1988) on chemical weathering rates. No significant correlation is obtained with any of the following morphometric parameters: mean elevation (Pinet and Souriau, 1988), maximum–minimum basin elevation (basin relief) and mean river slope (Summerfield and Hulton, 1994).

As an example, we reported in Fig. 7c the relationship between weathering rates and basin relief. This result, showing that silicate chemical weathering is not very sensitive to relief is the same as that stated by previous authors for total rock chemical weathering (Pinet and Souriau, 1988; Summerfield and Hulton, 1994) in large basins.

### 6.4. Relation with physical denudation

Continents weather both chemically and physically. The physical (or mechanical) denudation of continents consists in the transport of solids from soils and rocks by winds and continental waters. River suspended load are classically used to provide estimate of mechanical denudation. This idea suffers from two main limitations. For recent times, human impact perturbed river suspended load, either increasing it (e.g., under the influence of agriculture), or decreasing it (e.g., by sediment trapping in dams). The other ('natural') limitation was pointed out by Milliman and Meade (1983). Sediments eroded from highlands are likely to be deposited in lowland areas, floodplain or other natural reservoirs and never reach the sea. For these reasons the actual river suspended load imperfectly reflects the rate of modern physical denudation rates. With these limitations in mind, we used the data of river suspended load of Meybeck and Ragu (1997) to explore the relations between chemical weathering rates of silicates and their physical denudation. Suspended river material is mainly constituted of clays and oxides originating from the weathering of aluminosilicates. For consistency, the same normalization as that performed for chemical



weathering rates has been applied to physical erosion rates.

An interesting positive correlation appears between chemical weathering rates and physical weathering rates (Fig. 7d). The Don (having a very low physical erosion rate), and the Nile and Huanghe rivers (having relatively high physical weathering rates) have been excluded from Fig. 7d. We suggest that this correlation acts in favor of a coupling between physical and chemical erosion of silicates and indicates on a global scale, a strong control of chemical denudation by physical denudation. It means that the regions of the world where physical processes of erosion are active, are also the regions where aluminosilicates dissolve at the highest rate, and where CO<sub>2</sub> consumption by silicate weathering is the most important. For the global C cycle, this control of chemical processes by physical processes of erosion ascribes importance to the regions where mechanical denudation is high. A similar statement is reached by Edmond and Huh (1997) but contrasts with the conclusions of White and Blum (1995) for small rivers draining silicates, who concluded that the effects of physical erosion are of secondary importance with respect to climate (both runoff and temperature). The immediate question is then: as mountains are the preferential loci of physical denudation (Pinet and Souriau, 1988; Summerfield and Hulton, 1994), why is the correlation of chemical weathering rates and relief not more apparent? Although we have no definite answer to this issue, it is probable that the relief parameters tested above (which are the classically used) imperfectly reflect the mechanical ‘erodability’ of the continents. In addition, parameters such as lithology, induration of bedrock, abrupt temperature changes, freezing or glacial erosion are probably important for the production of fine material available to chemical weathering. The correlation reported here between physical and chemical denudation of silicates can be seen as a sort of mixing line between two extreme regimes of weathering, as described by geomorphologists: the transport limited and weathering limited regimes. In transport limited regimes, physical denudation is low and leads to an excess of soil formation that limits bedrock weathering. This effect of ‘soil shielding’ has been outlined by many authors at different scales: Stallard and Edmond (1987) for the Amazon, Ed-

mond et al. (1994) for the Orinoco, Bluth and Kump (1994) for small Hawaiian rivers and Gaillardet et al. (1995) for the Congo rivers and explains why, in spite of its optimal climatic conditions, the Zaire river has low rates of chemical weathering. The lowland areas of large river basins are probably exposed to this type of weathering regime. By contrast, in the weathering limited regime, soils are thin due to a high rate of mechanical denudation. The residence time of secondary products of weathering is much lower, chemical weathering of minerals is less intense, but the high physical rates continuously create new mineral surfaces what in fine enhances chemical weathering fluxes. An underlying theme of large scale weathering studies, that probably now needs further work, is the relation between fluxes and intensities of weathering. To explore more fully this concept of coupling between chemical dissolution and physical removal of soils, a comparison of silicate weathering rates and river suspended sediment chemistry for the largest rivers is attempted in a future paper (Gaillardet et al., 1999).

## 7. Some conclusions and perspectives

- The mixing model constructed in this paper and solved by an inversion method requires estimates of the chemical signature of waters draining the main lithologies: granitoid rocks from upper continental crust, basaltic rocks, carbonates and evaporites. Based on the available literature on the chemistry of small streams draining upper continental rocks, we favored in this paper the following set of Na-normalized molar ratio for the granitic silicate end member: Ca/Na =  $0.35 \pm 0.15$ , Mg/Na =  $0.24 \pm 0.12$ , HCO<sub>3</sub>/Na =  $2 \pm 1$ , 1000\*Sr/Na =  $3 \pm 1$ . This study is clearly a first order approach in which we assume that the chemical composition of the dissolved load derived from crustal rock weathering does not change too much from one large basin to another. Future local studies will be necessary to refine this working hypothesis.

- The result of the mixing model is that the present-day weathering rate of Na, K, Ca and Mg aluminosilicates on the continents is  $550 \times 10^6$  t yr<sup>-1</sup>, or 26% of the total flux of dissolved material transported by rivers to the oceans. The atmospheric

CO<sub>2</sub> consumption resulting from silicate weathering on the continents is found to be 0.104 Gt C yr<sup>-1</sup>. We show that recent estimates of weathering rates of rivers draining oceanic islands and volcanic arcs lead to a flux of consumed CO<sub>2</sub> by the weathering of young volcanics of 0.036 Gt C yr<sup>-1</sup>, i.e., more than 30% of the continental CO<sub>2</sub> consumption. Considering that only the weathering of Ca and Mg silicates is important for the global C cycle and climate regulation, we estimate a flux of consumed CO<sub>2</sub> of 0.058 Gt C yr<sup>-1</sup>. This flux seems almost five times lower than the flux of organic carbon (derived from biological consumption on the continents) transported by rivers. This tends to ascribe a minor importance to silicate weathering compared to net photosynthesis for the uptake of CO<sub>2</sub> from the atmosphere. Clearly, we need more data, in particular on basalt weathering for the main geodynamic contexts under different climates.

- As the total basin area of large rivers is never entirely underlain by silicate crustal rocks, the calculation of silicate weathering rates per unit area for the largest rivers is not easy. An attempt has been made to correct from this surface area effect and the control by several potentially controlling parameters has been explored. Runoff acts positively on silicate weathering, but our results do not allow to deduce a general relation between runoff and weathering rates. We suggest that the classical log–log correlations of weathering rates with runoff must be considered with care and do not contain any pertinent information when the slope is not significantly different from 1. Weathering rates show a reasonable correlation with average temperature only if we discard some rivers having abnormally low chemical weathering rates in spite of optimum climatic conditions. Finally, a positive correlation is observed between chemical weathering rates of silicates and physical weathering rates, calculated using suspended sediment loads. This correlation supports the idea that the physical removal of soils sustains chemical weathering by continuously refreshing mineral surfaces and by precluding the development of thick soils. For the global C cycle, this gives importance to regions where rocks and soils are mechanically fragile. A major difficulty of comparing chemical and physical weathering of silicates is that the suspended load of rivers imperfectly reflects the physical denudation of continental

rocks, in particular because of sediment storage within large basins. More work, particularly at local scales, is needed to examine the coupling between physical and chemical processes of silicate erosion.

## Acknowledgements

We are grateful to Michel Meybeck who provided us the chemical data set. We thank S. Gislason, P. Amiotte-Suchet and an anonymous reviewer for their helpful comments and criticisms. S. Levasseur is thanked for critical comments and N. Whiteley for English corrections. This is IGP contribution n° [] and INSU contribution n° [].

## References

- Allègre, C.J., Lewin, E., 1989. Chemical structure and history of the Earth: evidence from global non-linear inversion of isotopic data in a three-box model. *Earth Planet. Sci. Lett.* 96, 61–88.
- Allègre, C.J., Lewin, E., 1995. Scaling laws and geochemical distributions. *Earth Planet. Sci. Lett.* 132, 1–13.
- Allègre, C., Dupré, B., Gaillardet, J., Négrel, P., 1996. Sr–Nd–Pb isotopes systematics in Amazon and Congo. *Chem. Geol.* 131, 93–112.
- Amiotte-Suchet, P., Probst, J.L., 1993. Flux de CO<sub>2</sub> atmosphérique consommé par altération chimique continentale. Influence de la nature de la roche. *C.R. Acad. Sci. Paris* 317, 615–622, Série II.
- Amiotte-Suchet, P., Probst, J.L., 1995. A global model for present-day atmospheric/soil CO<sub>2</sub> consumption by chemical erosion of continental rocks (GEM-CO<sub>2</sub>). *Tellus* 47B, 273–280.
- Benedetti, M.F., Ménard, O., Noack, Y., Carvalho, A., Nahon, D., 1994. Water–rock interactions in tropical catchments: field rates of weathering and biomass impact. *Chem. Geol.* 118, 203–220.
- Berner, R.A., 1994. Geocarb II: a revised model of atmospheric CO<sub>2</sub> over Phanerozoic time. *Am. J. Sci.* 294, 56–91.
- Berner, E.K., Berner, R.A., 1996. *Global Environment: Water, Air and Geochemical Cycles*. Prentice-Hall, Upper Saddle River, NJ, 376 pp.
- Berner, R.A., Lassaga, A.C., Garrels, R.M., 1983. The carbonate–silicate geochemical cycle and its effect on atmospheric carbon dioxide over the past 100 million years. *Am. J. Sci.* 284, 1183–1192.
- Bluth, G.J.S., Kump, L.R., 1994. Lithological and climatological controls of river chemistry. *Geochim. Cosmochim. Acta* 58, 2341–2359.

- Brady, P.V., Carroll, S.A., 1994. Direct effects of CO<sub>2</sub> and temperature on silicate weathering: possible implications for climate control. *Geochim. Cosmochim. Acta* 58, 1853–1863.
- Buhl, D. et al., 1991. Nature and nurture: environmental isotope story of the River Rhine. *Naturwissenschaften* 78, 337–346.
- Burke, W.H. et al., 1982. Variations of seawater <sup>87</sup>Sr/<sup>86</sup>Sr throughout Phanerozoic time. *Geology* 10, 516–519.
- Cameron, E.M., Hall, G.E.M., J., V., R., K.H., 1995. Isotopic and elemental hydrogeochemistry of a major river system: Fraser river, British Columbia, Canada. *Chem. Geol. (Isotope Geo-science Section)* 122, 149–169.
- Chakrapani, G.J., Subramanian, V., 1990. Rates of erosion and sedimentation in the Mahanadi River Basin, India. *Chem. Geol.* 81, 241–253.
- Chhabra, R., 1996. Soil salinity and Water Quality. Brookfield, 284 pp.
- Douglas, G.B., Gray, C.M., Hart, B.T., Beckett, R., 1995. A strontium isotopic investigation of the origin of suspended particulate matter (SPM) in the Murray–Darling River System, Australia. *Geochim. Cosmochim. Acta* 59, 3799–3815.
- Dunne, T., 1978. Rates of chemical denudation of silicate rocks in tropical catchments. *Nature* 274, 244–246.
- Edmond, J.M., Huh, Y., 1997. A critique of geochemical models of the Cenozoic/Phanerozoic evolution of atmospheric pCO<sub>2</sub>. *Review of Geophysics*, in press.
- Edmond, J.M. et al., 1994. Fluvial geochemistry and denudation rate of Guyana Shield. *Geochim. Cosmochim. Acta* 59, 3301–3325.
- Edmond, J.M., Palmer, M.R., Measures, C.I., Brown, E.T., Huh, Y., 1996. Fluvial geochemistry of the northeastern Andes and its fordeep in the drainage of the Orinoco in Columbia and Venezuela. *Geochim. Cosmochim. Acta* 60 (16), 2949–2976.
- Flintrop, C. et al., 1996. Anatomy of pollution: rivers of North Rhine–Westphalia, Germany. *Am. J. Sci.* 296, 59–98.
- France-Lanord, C., Derry, L.A., 1997. Organic carbon burial forcing of the carbon cycle from the Himalayan erosion. *Nature* 390 (6), 65–67.
- Frape, S.K., Fritz, P., 1981. The chemistry and isotopic composition of saline groundwaters from the Sudbury Basin, Ontario. *Can. J. Earth Sci.* 19, 645–661.
- Gaillardet, J., Dupré, B., Allègre, C.J., 1995. A global geochemical mass budget applied to the Congo Basin rivers: erosion rates and continental crust composition. *Geochim. Cosmochim. Acta* 59 (17), 3469–3485.
- Gaillardet, J., Dupré, B., Allègre, C.J., 1997. Chemical and physical denudation in the Amazon river basin. *Chem. Geol.* 142, 141–173.
- Gaillardet, J., Dupré, B., Allègre, C.J., 1999. Geochemistry of large river suspended sediments: global silicate weathering or recycling tracer? *Geochim. Cosmochim. Acta*. Accepted for publication.
- Garrels, R.M., Mackenzie, F.T., 1971. *Evolution of Sedimentary Rocks*. Norton, New York.
- Gislason, S.R., Arnorsson, S., Armannsson, H., 1996. Chemical weathering of basalt in southwest iceland: effects of runoff, age of rocks and vegetative/glacial cover. *Am. J. Sci.* 296, 837–907.
- Goldstein, S.J., Jacobsen, S.B., 1987. The Nd and Sr isotopic systematics of river water suspended material: implications for crustal evolution. *Earth Planet. Sci. Lett.* 87, 249–265.
- Gordeev, V.V., Sidorov, I.S., 1993. Concentrations of major elements and their outflow into the Laptev Sea by the Lena river. *Mar. Chem.* 43, 34–45.
- Herczeg, A.L., Simpson, H.J., Mazor, E., 1993. Transport of soluble salts in a large semiarid basin: River Murray, Australia. *J. Hydrol.* 144, 59–84.
- Hieronymus, B., et al., 1995. *Chimie du fleuve Tocantins et des rivières côtières de l'Est du Para (Brésil)*. In: Olivry, J.C., Boulègue, J., (Eds.), *Grands Bassins Fluviaux*. ORSTOM Editions.
- Holland, H.D., 1978. *The Chemistry of Oceans and Atmosphere*. Wiley, New York.
- Krishnaswami, S., Trivedi, J.R., Sarin, M.M., Ramesh, R., Sharma, K.K., 1992. Sr isotopes and Rb in the Ganga–Brahmaputra river system: weathering in the Himalaya, fluxes to the Bay of Bengal and contributions to the evolution of oceanic <sup>87</sup>Sr/<sup>86</sup>Sr. *Earth Planet. Sci. Lett.* 109, 243–253.
- Livingstone, D.A., 1963. Chemical composition of rivers and lakes. 440 G, USGS pof. paper.
- Louvat, P., 1997. *Etude géochimique de l'érosion fluviale d'îles volcaniques à l'aide des éléments majeurs et traces*. Thesis Université Paris 7, 322 pp.
- Louvat, P., Allègre, C.J., 1997. Present denudation rates at Réunion island determined by river geochemistry: basalt weathering and mass budget between chemical and mechanical erosions. *Geochim. Cosmochim. Acta* 61 (17), 3645–3669.
- Ludwig, W., Probst, J.L., Kempe, S., 1996. Predicting the oceanic input of organic carbon by continental erosion. *Global Biochem. Cycles* 10 (1), 23–41.
- Meybeck, M., 1979. Concentrations des eaux fluviales en éléments majeurs et apports en solution aux océans. *Rev. Geol. Dyn. Geogr. Phys.* 21 (3), 215–246.
- Meybeck, M., 1984. *Les fleuves et le cycle géochimique des éléments*. Science Thesis, Paris 6, 558 pp.
- Meybeck, M., 1986. Composition des ruisseau non pollués de France. *Sci. Geol. Bull.* 39, 3–77.
- Meybeck, M., 1987. Global chemical weathering of surficial rocks estimated from river dissolved loads. *Am. J. Sci.* 287, 401–428.
- Meybeck, M., Ragu, A., 1997. *River Discharges to the Oceans: An Assessment of Suspended Solids, Major Ions and Nutrients*. 245 pp., in press.
- Milliman, J.D., Meade, R.H., 1983. World-wide delivery of river sediments to the oceans. *J. Geol.* 1, 1–21.
- Milliman, J.D., Syvitski, P.M., 1992. Geomorphic/tectonic control of sediment discharge to the ocean: the importance of small mountainous rivers. *J. Geol.* 100, 524–544.
- Négrel, P., Allègre, C.J., Dupré, B., Lewin, E., 1993. Erosion sources determined by inversion of major and trace element ratios in river water: the Congo Basin case. *Earth Planet. Sci. Lett.* 120, 59–76.
- Palmer, R., Edmond, J.M., 1989. The strontium isotope budget of the modern ocean. *Earth Planet. Sci. Lett.* 92, 11–26.
- Pande, K., Sarin, M.M., Trivedi, J.R., Krishnaswami, S., Sharma, K.K., 1994. The Indus River system (India–Pakistan): major-

- ion chemistry, uranium and Sr isotopes. *Chem. Geol.* 116, 245–259.
- Pinet, P., Souriau, M., 1988. Continental erosion and large-scale relief. *Tectonics* 7 (3), 563–582.
- Probst, J.L., Mortatti, J., Tardy, Y., 1994. Carbon river fluxes and weathering CO<sub>2</sub> consumption in the Congo and Amazon River Basins. *Appl. Geochem.* 9, 1–13.
- Ramanathan, A.L., Vaithyanathan, P., Subramanian, V., Das, B.K., 1994. Nature and transport of the solute load in the Cauvery river basin, India. *Water Resources*.
- Reeder, S.W., Hitchon, B., Levinson, A.A., 1972. Hydrogeochemistry of the surface waters of the Mackenzie River Drainage Basin, Canada: 1. Factors controlling inorganic compositions. *Geochim. Cosmochim. Acta* 26, 825–865.
- Roy, S., Gaillardet, J., Dupré, B., J., A.C., 1996. Strontium isotope geochemistry of the large rivers of China. Implication for weathering rates. Goldschmidt Conference, Heidelberg.
- Roy, S., Gaillardet, J., Allègre, C.J., 1999. Geochemistry of dissolved and suspended loads of the Seine River, France: anthropic impact, carbonate and silicate weathering. *Geochim. Cosmochim. Acta*, in press.
- Sarin, M.M., Krishnaswami, S., Dilli, K., Somayajulu, B.L.K., Moore, W.S., 1989. Major ion chemistry of the Ganga–Brahmaputra river system: weathering processes and Acta processes and fluxes to the Bay of Bengal. *Geochim. Cosmochim. Acta* 53, 997–1009.
- Stallard, 1980. Major elements geochemistry of the Amazon River system. PhD Thesis. MIT/Woods Hole Oceanographic Inst., WHOI-80-29.
- Stallard, R.F., Edmond, J.M., 1987. Geochemistry of the Amazon: 3. Weathering chemistry and limits to dissolved inputs. *J. Geophys. Res.* 92, 8293–8302.
- Stordal, M.C., Wassberg, G.J., 1983. Sm–Nd and Rb–Sr measurements on river water, suspended load and sediment from the Mississippi delta. *EOS Trans. Am. Geophys. Union* 64, 1064.
- Summerfield, M.A., Hulton, N.J., 1994. Natural controls of fluvial denudation rates in major world drainage basins. *J. Geophys. Res.* 99 (B7), 13871–13883.
- Taylor, S.R., McLennan, S.M., 1985. *The Continental Crust: its Composition and Evolution*. Blackwell, London, 312 pp.
- Wadleigh, M.A., Veizer, J., Brooks, C., 1985. Strontium and its isotopes in Canadian rivers: fluxes and global implications. *Geochim. Cosmochim. Acta* 49, 1727–1736.
- White, A.F., Blum, A.E., 1995. Effects of climate on chemical weathering in watersheds. *Geochim. Cosmochim. Acta* 59 (9), 1729–1747.
- Wollast, R., Mackenzie, F.T., 1983. The global cycle of silica. In: Aston, S.E. (Ed.), *Silicon Geochemistry and Biogeochemistry*. Academic Press, London, pp. 39–76.
- Yang, C.K., Telmer, K., Veizer, J., 1996. Chemical dynamics of the 'St. Lawrence' riverine system:  $\delta D_{H_2O}$ ,  $\delta^{18}O_{H_2O}$ ,  $\delta C_{DIC}$ ,  $\delta^{34}S_{sulfate}$  and dissolved  $^{87}Sr/^{86}Sr$ . *Geochim. Cosmochim. Acta* 60, 851–866.